



**Michigan  
Technological  
University**

Michigan Technological University  
**Digital Commons @ Michigan Tech**

---

Dissertations, Master's Theses and Master's Reports

---

2023

## **Chemical Decomposition of Flexible Polyurethane Foam to Generate a Media for Microbial Upcycling**

Kaushik Baruah

*Michigan Technological University, kbaruah@mtu.edu*

Copyright 2023 Kaushik Baruah

---

### **Recommended Citation**

Baruah, Kaushik, "Chemical Decomposition of Flexible Polyurethane Foam to Generate a Media for Microbial Upcycling", Open Access Master's Thesis, Michigan Technological University, 2023.

<https://doi.org/10.37099/mtu.dc.etr/1558>

Follow this and additional works at: <https://digitalcommons.mtu.edu/etr>



Part of the [Biochemical and Biomolecular Engineering Commons](#), [Polymer Chemistry Commons](#), and the [Polymer Science Commons](#)

CHEMICAL DECOMPOSITION OF FLEXIBLE POLYURETHANE FOAM TO  
GENERATE A MEDIA FOR MICROBIAL UPCYCLING

By

Kaushik Baruah

A THESIS

Submitted in partial fulfillment of the requirements for the degree of

MASTER OF SCIENCE

In Chemical Engineering

MICHIGAN TECHNOLOGICAL UNIVERSITY

2023

© 2023 Kaushik Baruah

This thesis has been approved in partial fulfillment of the requirements for the Degree of  
MASTER OF SCIENCE in Chemical Engineering.

Department of Chemical Engineering

Thesis Advisor: *Dr. Rebecca Ong*

Committee Member: *Dr. David Shonnard*

Committee Member: *Dr. Patricia Heiden*

Department Chair: *Dr. Pradeep Agrawal*

# Table of Contents

List of Figures .....	v
List of Tables .....	viii
Author Contribution Statement.....	ix
Acknowledgements.....	x
List of Abbreviations .....	xi
Abstract .....	xii
1 Introduction.....	1
1.1 Polyurethane Foam and the Current Market .....	1
1.2 Chemistry of Polyurethane Foam.....	2
1.2.1 Rigid Polyurethane Foam (RPUF).....	3
1.2.2 Flexible Polyurethane Foam (FPUF) .....	4
1.3 Polyurethane Waste Problem and Recycling .....	5
1.3.1 Mechanical Recycling.....	6
1.3.2 Thermal Recycling.....	6
1.3.3 Chemical Recycling.....	7
1.3.3.1 Hydrolysis.....	8
1.3.3.2 Glycolysis .....	9
1.3.3.3 Ammonolysis .....	9
1.3.3.4 Predicted Decomposition Mechanisms.....	10
1.4 Microbial Upscaling .....	13
1.5 Project Objectives.....	13
2 Materials and Methods.....	15
2.1 Materials .....	15
2.2 Methods .....	15
2.2.1 Preparation of FPUF .....	15
2.2.2 Thermogravimetric Analysis .....	16
2.2.3 FPUF Decomposition in Batch Reactor.....	16
2.2.4 FPUF Decomposition in a Continuous Stirred-Tank Reactor .....	17
2.2.5 FTIR and NMR Scans.....	18
2.2.6 Microbial Upcycling with FPUF Liquid.....	18
2.2.7 Microbial Upcycling with Standard Chemical Media .....	19
2.2.8 DNA Analysis.....	20
3 Results and Discussion .....	22
3.1 Thermogravimetric Analysis.....	22
3.2 Solubilization of FPUF in NH <sub>4</sub> OH.....	22
3.2.1 Batch Reactor.....	22

3.2.2	Continuously Stirred-Tank Reactor .....	23
3.2.3	Effect of Higher Solids Loading of FPUF .....	24
3.3	FTIR and NMR Analysis .....	25
3.4	Upcycling of Microbial Consortia.....	27
3.5	Relative Abundance of Microbial Communities and Species.....	30
4	Conclusions and Recommendations .....	34
5	Reference List .....	36
6	Appendix.....	44
6.1	Solubilization Data of FPUF in NH <sub>4</sub> OH .....	44
6.1.1	Batch Reactor Run Data.....	44
6.1.2	Parr Reactor Run Data .....	45
6.1.3	Higher Solids Loading Experimental Data .....	46
6.2	Microbial Growth Data (OD <sub>600</sub> ).....	47
6.2.1	OD <sub>600</sub> During Incubation Period of Microbial Consortia in FPUF Media with 2.3 g/L Dissolved Carbon Products .....	47
6.2.2	OD <sub>600</sub> During Incubation Period of Microbial Consortia in FPUF Liquid Media with 8.8 g/L Dissolved Carbon Products.....	48
7	Copyright Documentation.....	49

## List of Figures

Figure 1.1: Polyurethane repeating unit containing carbon chains (R and R') joined by urethane linkage (-NHCO). .....	1
Figure 1.2: Market demand of Polyurethane foams (FPUF and RPUF), and other PU products <sup>13</sup> . .....	2
Figure 1.3: Reaction between the isocyanate and hydroxyl groups to form a urethane link between the two carbon chains, R and R'. .....	2
Figure 1.4: Most commonly used diisocyanates for polyurethane foam production include 2,4-toluene diisocyanate (TDI), 4,4'-methylenediphenyl diisocyanate (MDI), and 1,6-hexamethylene diisocyanate (HDI). .....	3
Figure 1.5: Reaction between diols and commonly used diisocyanates (a) MDI, and (b) TDI to form the respective polyurethane CRUs. ....	3
Figure 1.6: Closed-cell structure of rigid polyurethane foam (RPUF) <sup>20</sup> . ....	4
Figure 1.7: Open-celled structure of flexible polyurethane foam (FPUF) <sup>20</sup> . ....	4
Figure 1.8: In the U.S. in 2016, 52% of the total PUF inflow was disposed of, while only 10% was recycled mechanically <sup>28</sup> . ....	5
Figure 1.9: Polyurethane foam is fed into a roll mill to produce a powder-like material to be used as fillers in new polyurethane products. ....	6
Figure 1.10: Hydrolysis of polyurethane foam forms amines, polyols, and CO <sub>2</sub> . ....	8
Figure 1.11: Glycolysis reaction of polyurethane with ethylene glycol forms a peroxy acid and alcohol <sup>54</sup> . ....	9
Figure 1.12: Decomposition of flexible polyurethane foam via ammonolysis using supercritical ammonia <sup>59</sup> . ....	10
Figure 1.13: Decomposition mechanism of flexible polyurethane foam (FPUF) via combined ammonolysis and hydrolysis to form carbamic acid, 4,4'-methylenediphenyldiamine (MDA), and a polyol mixture. ....	11
Figure 1.14: Base-catalyzed hydrolysis mechanism of flexible polyurethane foam (FPUF) to form a mixture of carboxylic acids and 4,4'-methylenediphenyldiamine (MDA). ....	12
Figure 1.15: Process flowchart of the experimental process. ....	14
Figure 2.1: Flexible polyurethane foam (FPUF) shredded using a paper shredder. ..	15
Figure 2.2: Cryo-milled flexible polyurethane foam (FPUF) used for thermogravimetric analysis. ....	16
Figure 2.3: Batch reactor assembly with reactor head attached to the reactor body using metal clamps. The reactor body is covered with heating tape. ....	16

Figure 3.1: Thermogravimetric scan of flexible polyurethane foam (FPUF) shows a 2-step thermal decomposition. The sample starts decomposing at 210°C followed by a second decline in the weight percent at 400°C. ....	22
Figure 3.2: Flexible polyurethane foam (FPUF) solubilization in a custom batch reactor increased with temperature and time to a maximum of 53% for 62.5 g FPUF/L 16% NH <sub>4</sub> OH. Error bars represent the average ± standard deviation (n=3). ....	23
Figure 3.3: Flexible polyurethane foam (FPUF) solubilization in a Parr reactor increased with temperature and time to a maximum of 95% for 62.5 g FPUF/L 16% NH <sub>4</sub> OH. Error bars represent the average ± standard deviation (n=3). ....	24
Figure 3.4: Percent of FPUF solubilized in ammonium hydroxide remains above 90% until a solids loading of 30% FPUF. Error bars represent average ± standard deviation. ....	24
Figure 3.5: Residual solid particles from FPUF ammonolysis after filtration and oven drying at 55°C. Reaction conditions: 200°C, 200 psi, 30 minutes for 25% solids loading (g FPUF per mL NH <sub>4</sub> OH) at 60 rpm. ....	25
Figure 3.6: FTIR spectra of original FPUF sample and decomposed solid obtained after product filtration shows the decomposition of urethane bonds after the reaction. ....	25
Figure 3.7: Liquid product obtained from flexible polyurethane foam (FPUF) decomposition at 25% solids loading (g FPUF/mL 16% NH <sub>4</sub> OH) in a Parr reactor at 200°C, 30 min, and 60 RPM. ....	26
Figure 3.8: <sup>13</sup> C NMR analysis of the obtained liquid product and predicted carbon source, 2,4-toluenediamine for microbial growth. ....	27
Figure 3.9: Optical density (OD <sub>600</sub> ) found to be lower for microbial consortia (Laura 1, Laura 2, and Emma 2) in Bushnell Haas media with FPUF concentrations of (a) 2.3 g/L and (b) 8.8 g/L. Error bars represent average ± standard deviation (n=3). ....	28
Figure 3.10: Standard chemicals 2,4-toluenediamine (TDA), 4,4'-methylenedianiline (MDA), and polypropylene glycol (PPG) used for microbial upcycling experiments. ....	29
Figure 3.11: (a) Laura 1 and (b) Laura 2 cultures show no growth in FPUF media or any of the standard chemicals at a mass concentration of 8.8 g/L, while (c) Emma 2 shows slight growth in FPUF media, 2,4-toluenediamine (TDA), and 4,4'-methylenedianiline (MDA). PPG = polypropylene glycol. Error bars represent average ± standard deviation (n=3). ....	29
Figure 3.12: Microbial consortia (a) Laura 1, (b) Laura 2, and (c) Emma 2 show high growth in 1,2-Propanediol (PDO) and 1,4-Butanediol (BDO) as compared to other standard chemicals. All compounds were added as the sole carbon	

source at 8.8 g/L in BH media. TDA = 2,4-toluenediamine (TDA); MDA = 4,4'-methylenedianiline; PPG = polypropylene glycol. Error bars represent avg $\pm$ sd (n=3). .....	30
Figure 3.13: Genus taxa plot of microbial communities before and after the incubation period shows the change in relative abundance of microbial communities over time. ....	31
Figure 3.14: Species classification plot indicates the possible ability of <i>Brevundimonas diminuta</i> and <i>Chelatococcus daeguensis</i> present in Laura 1 and Emma 2 cultures to metabolize 2,4-toluenediamine (TDA) present in FPUF liquid media. ....	33



## List of Tables

Table 1.1: Yield (wt%) from the pyrolysis of polyurethane foam in a Pyroprobe-1000 + secondary reactor compared to a laboratory furnace <sup>40</sup> . .....	7
Table 2.1: Mass of standard chemicals added to prepare media for microbial upcycling.	20
Table 2.2: Real-time thermocycler program for PCR plate reactions. ....	20
Table 3.1: <sup>13</sup> C NMR chemical shift and corresponding carbon environment. ....	27
Table 6.1: Solubilization triplicate data of FPUF reactions in a batch reactor. Reaction conditions: 30, 60 minutes; 140°C, 160°C, 180°C, 200°C; 16% w/w NH <sub>4</sub> OH; 6.25% FPUF in NH <sub>4</sub> OH. ....	44
Table 6.2: Solubilization triplicate data of FPUF reactions in a continuously stirred-tank reactor (Parr reactor). Reaction conditions: 30, 60 minutes; 140°C, 160°C, 180°C, 200°C; 60 rpm; 16% w/w NH <sub>4</sub> OH; 6.25% FPUF in NH <sub>4</sub> OH. ....	45
Table 6.3: Average solubilization data of FPUF decomposition reaction at higher solids loading. Reaction conditions: Reaction conditions: 60 minutes; 200°C; 60 rpm in a Parr reactor; 16% w/w NH <sub>4</sub> OH. ....	46
Table 6.4: OD <sub>600</sub> of microbial consortia in FPUF media. Media specifications: 52 mL media; 2.3 g/L dissolved carbon products; media neutralized to pH = 6.81. ....	47
Table 6.5: Table A.4: OD <sub>600</sub> of microbial consortia in FPUF media. Media specifications: 52 mL media; 8.8 g/L dissolved carbon products; media neutralized to pH = 6.75. ....	48

## **Author Contribution Statement**

Rebecca Ong designed and coordinated the overall project. Rebecca Ong designed the custom batch reactor apparatus. Sulihat Aloba taught the assembly and operation of the custom batch reactor system. Hunter Stoddard helped with the preparation of microbial seed cultures. Kaushik Baruah performed the solubilization reactions of flexible polyurethane foam, microbial upcycling experiments, and the DNA analysis process. Laura Schaerer isolated and cultured the Laura 1 and Laura 2 consortia used and helped analyze data in Rstudio. Emma Byrne isolated and cultured the Emma 2 consortia. Kaushik Baruah wrote the manuscript with input from Dr. Rebecca Ong. Dr. Rebecca Ong edited the manuscript.

## Acknowledgements

I would like to express my sincere gratitude to my advisor, Dr. Ong, for her invaluable support and guidance throughout the course of this project. Her constant encouragement, positive reinforcement, and insightful feedback have been instrumental in navigating the difficulties of research as a novice and complete this work. I am incredibly grateful for everything she has taught me over the past two years.

I am also thankful to Hunter Stoddard, Laura Schaerer, and Sulihat Aloba for their expertise and guidance during my experiments. They have always been eager to help me navigate experiments and answer questions. I would also like to thank Jerry Lutz from the Department of Chemistry at Michigan Technological University for teaching me how to operate and troubleshoot the Nuclear Magnetic Resonance spectrophotometer.

Lastly, I would like to express my appreciation to my parents Kabindra and Mousumee K. Baruah for their unwavering support throughout my academic journey. Their love and support have been the most important factor for my academic success. I would not be where I am today without their constant belief in me as a researcher since 12<sup>th</sup> grade.

## List of Abbreviations

PU – Polyurethane

PUF – Polyurethane Foam

FPUF – Flexible Polyurethane Foam

RPUF – Rigid Polyurethane Foam

CRU – Constitutional Repeating Unit

MDI – 4,4'-methylenediphenyl diisocyanate

TDI – 2,4-toluene diisocyanate

DMEA – Dimethylethanolamine

CHCA – Cyclohexane Carboxylic Acid

OSPW – Oil Sands Process-affected Waters

NA – Napthenic Acid

BH – Bushnell Haas

TDA – 2,4-toluenediamine

MDA – 4,4'-methylenedianiline

PPG – Polypropylene Glycol

PDO – 1,2-propanediol

BDO – 1,4-butanediol

TGA – Thermogravimetric Analysis

CSTR – Continuously Stirred-Tank Reactor

TAE – Tris Acetate EDTA

## Abstract

Polyurethane waste is becoming a global concern as a large amount is being disposed of in landfills every year, and only a fraction is being recycled. Several polyurethane recycling techniques exist, of which ammonolysis and base-catalyzed hydrolysis is the least explored. Flexible polyurethane foam (FPUF) decomposition can generate amines that can act as a carbon source for the growth of microbial consortia. This study aims to generate a novel media capable of microbial upcycling via ammonolysis and base-catalyzed hydrolysis of flexible polyurethane foams (FPUFs) using ammonium hydroxide and subsequently determine the reaction conditions for maximum solubilization of polyurethane foam in ammonium hydroxide.

Flexible polyurethane foam (FPUF) samples were decomposed using 16%  $\text{NH}_4\text{OH}$  at 6.25%, 10%, 15%, 20%, 25%, and 30% weight percent solids loading for a temperature range of 140°C-200°C with 20°C intervals. Residence times of 30 minutes and 60 minutes were tested. The effectiveness of the decomposition process was determined based on the solubilization of flexible polyurethane foam (FPUF) in ammonium hydroxide. The solid and liquid products were analyzed using FTIR and NMR spectroscopy, respectively, to determine the decomposed products. 2,4-toluenediamine (TDA) was identified as the carbon source in the liquid from the NMR spectra of the liquid product.

Microbial media prepared using the liquid product and possible decomposed products in Bushnell Haas broth was inoculated with three different microbial consortia – Laura 1, Laura 2, and Emma 2 in minimal Bushnell Haas media. Optical density measurements were taken during incubation to account for microbial growth. DNA analysis of microbial pellets collected from the incubated sample before and after incubation was conducted to identify specific microbial strains that could utilize decomposed polyurethane foam liquid for growth.

This work successfully achieved 95% solubilization of flexible polyurethane foam (FPUF) in  $\text{NH}_4\text{OH}$ . 2,4-toluenediamine (TDA), the major chemical used to make 2,4-toluene diisocyanate, which is used in the manufacture of polyurethanes, was identified as a product. Two microbial species - *Brevudimonas diminuta* and *Chelatococcus daeguensis* – were comparatively enriched when consortia were grown in media containing pure TDA or FPUF liquid. However, an initial increase in microbial growth in the PUF and TDA media within the first 24 hours was quickly followed by a reduction in  $\text{OD}_{600}$ , indicating either rapid depletion of the carbon source or generation of a toxic by-product. Future work will attempt to isolate the organisms that may be responsible for TDA metabolism and develop a method to quantify the amount of TDA in the liquid FPUF product.

# 1 Introduction

## 1.1 Polyurethane Foam and the Current Market

Polyurethane (PU) is a synthetic polymer comprised of repeating units of urethane groups (-NHCOO-) linked to carbon chains R and R' (**Figure 1.1**). Since its initial lab formulation in 1937, polyurethane (PU) has quickly grown to become one of the most commonly utilized polymers, with a steadily expanding global market<sup>1</sup>. Because of its sturdiness, flexibility, and resistance to chemicals and abrasion, polyurethane is the perfect material for many applications.

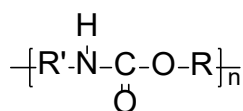


Figure 1.1: Polyurethane repeating unit containing carbon chains (R and R') joined by urethane linkage (-NHCO).

Polyurethanes (PUs) are typically used in building, packaging, insulation, footwear, bedding, upholstery, clothing, and car parts<sup>2</sup> and come in various formats. Rigid foams, flexible foams, coatings, adhesives and sealants, elastomers, etc., are all forms of polyurethane<sup>3</sup>. Rigid polyurethane foams (RPUFs) are mainly used as an insulating material in construction and refrigeration applications<sup>4</sup>. In contrast, flexible polyurethane foams (FPUFs) are primarily used as a cushioning material in transportation, furniture, packing, etc<sup>4</sup>. Exposed wooden surfaces can have glossy polyurethane coatings sprayed to prevent rust, repel water, and shield against UV rays, scratches, and stains<sup>5</sup>. Adhesives and sealants made using polyurethane are typically utilized in sealing/joining construction materials and pipework<sup>6</sup>. Polyurethane elastomers are extensively used as biomaterials<sup>7</sup>, shoe soles, gaskets, etc<sup>8</sup>.

Some advantages stand out when comparing polyurethane to more traditional materials like wood and metals, including its low density, low moisture permeability, low heat conductivity, high strength-to-weight ratio, and exceptional dimensional stability<sup>9</sup>. Furthermore, it is possible to obtain desired qualities for particular applications by modifying the formulation, reaction conditions, and use of additives during polyurethane synthesis.

In 2021, 24.72 million tons of polyurethane were produced globally<sup>10</sup>, and the market is expected to grow to 29.2 million tons by 2029<sup>11</sup>. The construction industry dominated the polyurethane market, accounting for 26% of total demand, while the furniture and interior design industry ranks second, accounting for 23% of the market in 2021<sup>12</sup>. In 2021, polyurethane foams (PUFs) accounted for 68% of the

polyurethane market, while elastomers, adhesives, sealants, coatings, etc., accounted for 32%<sup>13</sup> (**Figure 1.2**).

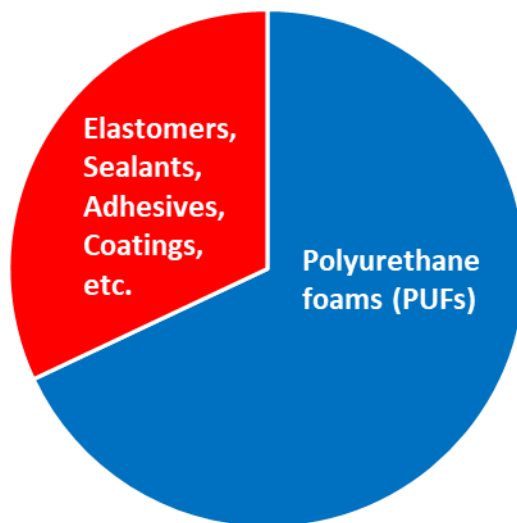


Figure 1.2: Market demand of Polyurethane foams (FPUF and RPUF), and other PU products<sup>13</sup>.

## 1.2 Chemistry of Polyurethane Foam

Isocyanates with more than one reactive isocyanate group (-NCO) per molecule and alcohols with two or more reactive hydroxyl (-OH) groups per molecule (diols, triols, polyols) combine exothermically to form polyurethane foam. **Figure 1.3** depicts the primary reaction, also called the gelling reaction, in which the isocyanate and hydroxyl groups combine to form a urethane group <sup>14</sup>.



Figure 1.3: Reaction between the isocyanate and hydroxyl groups to form a urethane link between the two carbon chains, R and R'.

Rigid and flexible polyurethane foams undergo a similar reaction, the only difference being in the monomers used. Highly cross-linked polyol monomers cause rigidity and lead to the formation of RPUFs, while long, flexible polyol chains form FPUFs<sup>15</sup>. Also, blowing agents control the foam cell structure and thus manipulate the rigidity and cell structure of the final foam product<sup>16</sup>. The diisocyanate segment is responsible for the reactivity and curing properties of PUF<sup>15</sup>, and they can be aliphatic or aromatic (**Figure 1.4**). The isocyanate ends are highly reactive; they

react with polyols of variable chain length to form the constitutional repeating unit (CRU) of PUFs<sup>17,18</sup> (**Figure 1.5**).

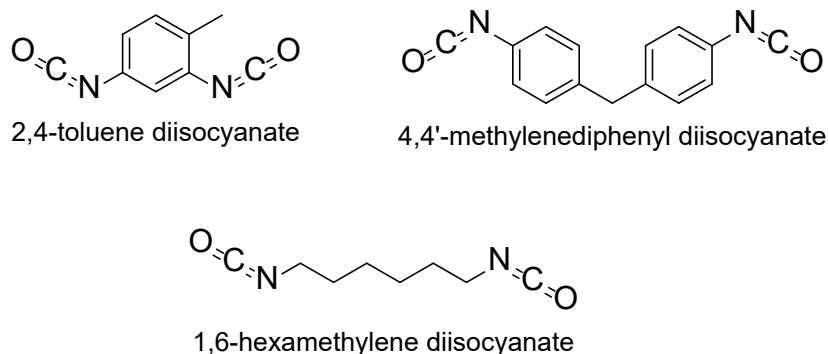


Figure 1.4: Most commonly used diisocyanates for polyurethane foam production include 2,4-toluene diisocyanate (TDI), 4,4'-methylenediphenyl diisocyanate (MDI), and 1,6-hexamethylene diisocyanate (HDI).

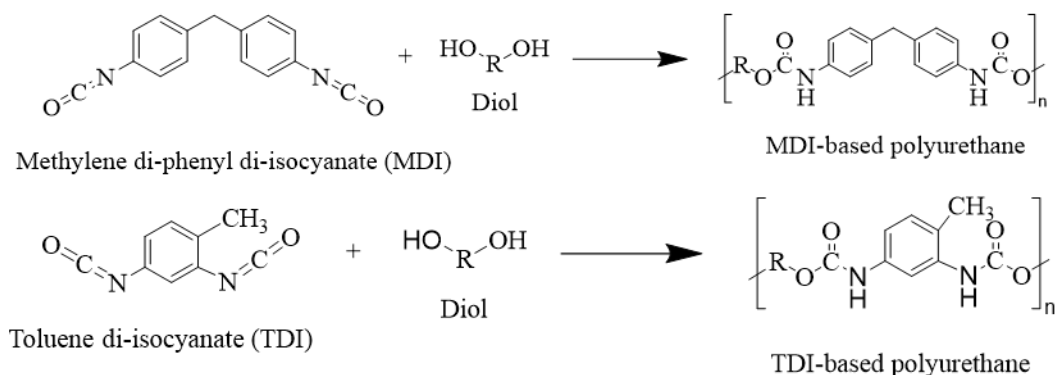


Figure 1.5: Reaction between diols and commonly used diisocyanates (a) MDI, and (b) TDI to form the respective polyurethane CRUs.

### 1.2.1 Rigid Polyurethane Foam (RPUF)

Rigid polyurethane foam (RPUF) is a highly cross-linked, low-density, thermoset material<sup>19</sup>. Rigid polyurethane foams (RPUFs) have a closed-cell structure and low porosity<sup>20</sup> (**Figure 1.6**). RPUFs possess excellent compressive and load-bearing capabilities and high tensile strength and elongation properties<sup>18</sup>. The hydroxyl value and functionality of the polyol monomer are used to determine the stoichiometry of the polymerization reaction. The hydroxyl value measures the concentration of free hydroxyl groups in a polyol. Typically, diols with a hydroxyl value greater than 200 mg KOH/g are used to manufacture RPUFs<sup>21</sup>. These diols react with diisocyanate (usually MDI or TDI) in the presence of a catalyst, foam



stabilizer, and other additives, such as fire retardants<sup>18</sup>. Generally, amine, organometallic, and inorganic salts of bismuth and zinc are used as catalysts to make polyurethane<sup>22</sup>. Non-hydrolyzable Si-C foam stabilizers are commonly used to make the final product more long-lasting<sup>23</sup>.

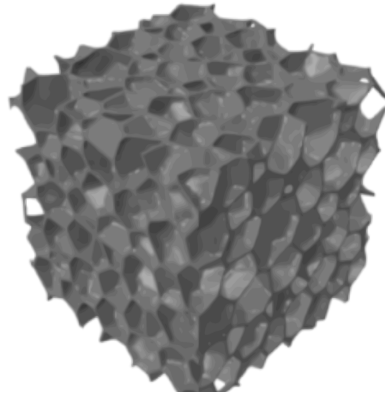


Figure 1.6: Closed-cell structure of rigid polyurethane foam (RPUF)<sup>20</sup>.

### 1.2.2 Flexible Polyurethane Foam (FPUF)

Compared to RPUF, flexible polyurethane foam (FPUF) is highly porous and has an open-cell structure<sup>24</sup> (**Figure 1.7**). FPUF is characterized by a cellular structure that permits some compression and resilience, creating a cushioning effect. This characteristic makes it a favored material in furniture, bedding, vehicle seats, sporting goods, packaging, footwear, and carpet padding. It is also vital for filtering and soundproofing<sup>25</sup>.

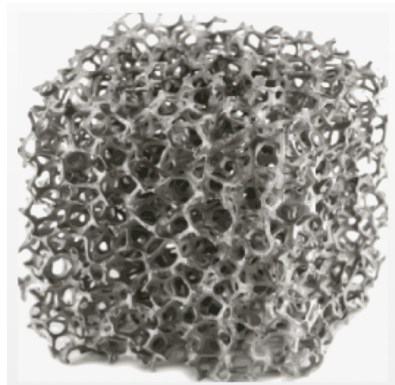


Figure 1.7: Open-celled structure of flexible polyurethane foam (FPUF)<sup>20</sup>.

Long-chain polyols with a hydroxyl value of 28-56 mg-KOH/g are reacted with diisocyanates (usually TDI or MDI) to produce FPUFs<sup>21</sup>. A smaller number of hydroxyl groups means a smaller number of sites for the isocyanate groups to bond

to, resulting in a weaker polymeric structure. Polyols with a molecular weight of 3000-4000 are commonly used to manufacture FPUFs. Stannous octanoate and N,N'-dimethylethanolamine (DMEA) are the two most commonly utilized catalysts in manufacturing flexible polyurethane foam (SnOct)<sup>26,27</sup>. A blowing agent such as water or a low boiling point organic liquid generates hollow cells inside the final foam; this makes it flexible<sup>18</sup>.

### 1.3 Polyurethane Waste Problem and Recycling

In 2016, the United States produced 2,900 thousand tonnes (kt) of polyurethane foam and imported 920 kt for consumption, 2,000 kt were disposed of as post-consumer trash<sup>28</sup>. A total of 390 kt PUF was recycled and released back onto the market as carpet underlayment, and the remaining 1,430 kt circulated in the hands of consumers as products<sup>28</sup> (**Figure 1.8**). If PU is left in the ecosystem unchecked, it has the potential to cause significant environmental issues. Treatment of aging polymeric materials has emerged as a global issue due to the massive output of polymeric wastes. Because they must be used in daily life and business, PUs end up in municipal solid waste systems (usually by discarding consumer and industrial products). These wastes frequently have a long lifespan and are durable (e.g., upholstered furniture, mattresses, automobile parts)<sup>29</sup>.

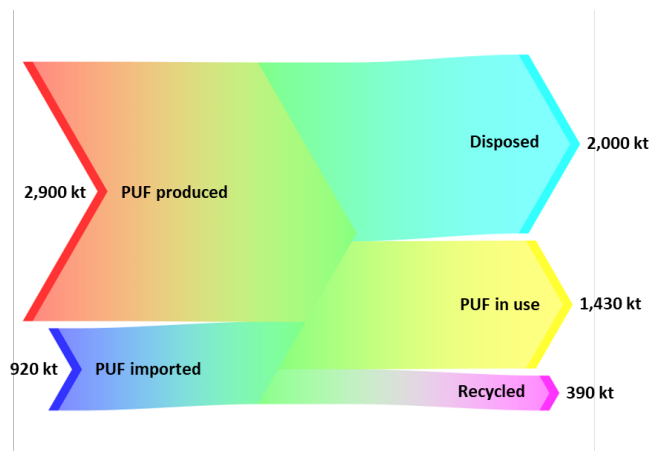


Figure 1.8: In the U.S. in 2016, 52% of the total PUF inflow was disposed of, while only 10% was recycled mechanically<sup>28</sup>.

Polyurethane foam waste is difficult to process and dispose of in landfills due to its low density and high volume. Additionally, incinerating it will release toxic carbon monoxide gas<sup>30</sup>. Increasing landfill prices and limited landfill space are pushing the investigation of alternate disposal methods for polyurethane products<sup>31</sup>. In response to the increasing production and consumption of PU materials, recycling and reuse have played an important role in waste reduction by transforming waste into value-added products, new chemicals, monomers, etc. Polyurethane recycling is gaining popularity across the world as a result of ongoing legislative and

environmental reforms. Polyurethane can be effectively recycled from various consumer items such as appliances, autos, mattresses, carpet cushions, and upholstered furniture<sup>32</sup>. There are three major ways to recycle waste PUFs, broadly classified into mechanical, thermal, and chemical recycling<sup>33</sup>.

### 1.3.1 Mechanical Recycling

The term "mechanical (physical) recycling of PU wastes" refers to one of the numerous types of particle recycling that includes regrinding, rebinding, adhesive pressing, injection molding, and compression molding<sup>29</sup>. Usually, the waste for this procedure comes from post-consumer items, factory trimmings, and leftovers from the production line. It entails converting solid trash into flakes, granules, or powder<sup>13</sup>. These materials can be utilized as stuffing for pillows, toys, and other items or as a substrate in later procedures.

Grinding, cutting, or ripping can all be used to create fragmentation. Two-roll mills produce fine powders (with particles smaller than 100-125 microns), as shown in **Figure 1.9**. The obtained powders can be employed as fillers in new polyurethanes<sup>34</sup>. To prepare powder with a greater particle diameter (125-250 microns)<sup>35</sup>, precision knife cutting is used. Pellet mills are used to make granules. They are made of two or more metal rollers that push the polyurethane through a metal plate with perforations. These recycling approaches are inefficient, and acquired items are low-quality, limiting the accessible sales markets<sup>30</sup>. Because of contamination or the inclusion of additional materials such as dirt, grease, food particles, etc., post-consumer waste goods cannot be used as stock for mechanical recycling<sup>30</sup>.

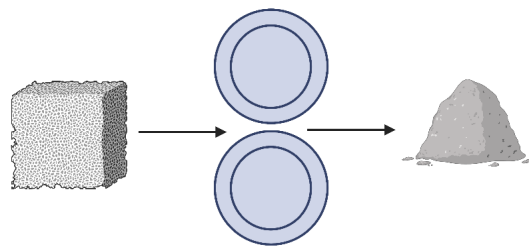


Figure 1.9: Polyurethane foam is fed into a roll mill to produce a powder-like material to be used as fillers in new polyurethane products.

### 1.3.2 Thermal Recycling

Most polyurethane products, such as low and high-density foam, are thermostable<sup>36</sup>. The material is distinguished by its lattice structure, which helps it maintain its shape and resistance under high-pressure and high-temperature conditions that

ultimately lead to degradation. As a result, after it has been manufactured and reaches the gelation point, the material cannot be melted or remodeled into other products<sup>37</sup>. Because of this, thermal recycling of polyurethanes is difficult and expensive.

Other writers have already investigated the pyrolysis and combustion processes of polyurethanes. Ketata et al.<sup>38</sup> found that a mixture of low molecular weight polyethers were released between 270°C to 700°C during the thermal decomposition of PUF (produced by the reaction between ethanediol and MDI) in air. CO and CO<sub>2</sub> accompanied this release at 320°C-660°C and 160°C-700°C, respectively<sup>38</sup>. Chao and Wang<sup>39</sup> investigated the influence of phosphorus and brominated fire retardants on the decomposition of polyurethane foam under air and nitrogen environments. They found that the foams began to decompose thermally between 300-400°C. Font et al.<sup>40</sup> thoroughly studied all the products formed after the pyrolysis of polyurethane foam. They obtained a yield of 32.3 wt% and 31.75 wt% after pyrolysis of polyurethane foam in a Pyroprobe-1000, followed by a secondary reactor and a laboratory furnace, respectively. The products constituted light hydrocarbon gases (**Table 1.1**). The purification of light hydrocarbons is a high-energy and cost-intensive process<sup>41</sup>. Even if the compounds obtained from the pyrolysis of polyurethane (**Table 1.1**) were to be separated, the cost involved in the entire process would be too high to make the process commercially viable<sup>42</sup>.

Table 1.1: Yield (wt%) from the pyrolysis of polyurethane foam in a Pyroprobe-1000 + secondary reactor compared to a laboratory furnace<sup>40</sup>.

Compound	Yield from Pyroprobe 1000 + secondary reactor (wt%)	Yield from Laboratory furnace (wt%)
Methane	5.3	7.0
Ethylene	11.2	14.0
Propene	1.2	0.84
Acetylene	0.5	0.81
1,3-Butadiene	0.5	1.3
Benzene	13.6	7.8

### 1.3.3 Chemical Recycling

Although mechanical recycling is more affordable, the finished product quality suffers since the foam degrades during the recycling process<sup>30</sup>. On the other hand, chemical recycling enables the recovery of the original components from which the foam was created, producing a recovered good of higher quality and better performance<sup>43</sup>. Chemical (or tertiary) recycling uses chemolytic processes to break down polymeric waste into monomers to manufacture virgin materials or generate alternative products like fuels<sup>44</sup>.

Chemical recycling methods can be classified as hydrolysis, glycolysis, and ammonolysis. Each of these chemical recycling processes has its advantages and disadvantages. The most suitable technique will depend on the specific properties of the foam and the desired end product. However, high cost and complexity of chemical recycling procedures prevent their mainstream use<sup>29</sup>. Additional research and development are required to scale and optimize them.

### 1.3.3.1 Hydrolysis

Hydrolysis was the first chemical technique to recycle polyurethane waste, particularly flexible foams<sup>35</sup>. Waste polyurethane reacts with water, either liquid or steam, to produce amines, polyols, and carbon dioxide<sup>45</sup> (**Figure 1.10**). The most important advantage of this method is that it can be used to recycle both production scraps and post-consumer waste<sup>34</sup>.

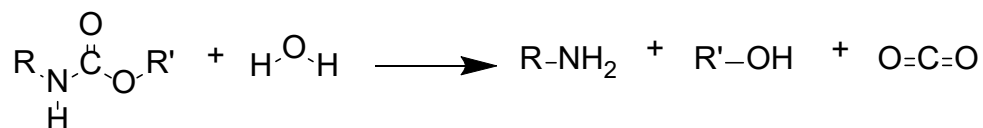


Figure 1.10: Hydrolysis of polyurethane foam forms amines, polyols, and CO<sub>2</sub>.

The procedure is carried out in an oxygen-free environment under high temperatures (150-320 °C)<sup>35</sup>. Hydrolysis degradation products can easily be separated using high-performance liquid chromatographic separation<sup>46</sup>. The resultant polyols can be utilized as additions to the original polyol in manufacturing polyurethane or as fuel. Furthermore, the recovered amine intermediates can be subjected to phosgene treatment to recover the initial isocyanates. Moreover, reacting hydrolyzed polyols with isocyanates regenerates the polyurethanes<sup>47</sup>. However, if commercial polyurethane containing fire retardants were to be recycled via hydrolysis, the residence time would be high due to the temperature resistance of the foam<sup>48</sup>. The most significant drawback of hydrolysis is that it demands a considerable energy input into the reactor, either to heat the batch or to apply high pressure, making this process uneconomical<sup>49</sup>. As a result, hydrolysis has yet to be converted onto a commercial scale. However, hydrolysis of FPUF using a base catalyst can marginally improve the efficiency of the process. In the presence of a quarternary ammonium salt or organic sulfonate, PUF is hydrolyzed relatively easily with a high yield<sup>50</sup>. The urethane bond in FPUF is cleaved by base-catalyzed hydrolysis, yielding low molecular weight glycols, diols, and diamines<sup>50</sup>. The only drawbacks of base-catalyzed hydrolysis are the slow rate at lower temperatures and undesired side reactions at higher temperatures.

### 1.3.3.2 Glycolysis

In glycolysis, the polyurethane chain is destroyed by consecutive transesterification reactions of the urethane bond with low molecular weight glycols in the presence of a catalyst<sup>51</sup>. The catalyst used significantly impacts the characteristics of the recovered products and the time required to degrade the foam completely<sup>52</sup>. Bases, including amines, hydroxides, and alkoxides, as well as Lewis acids, are utilized as catalysts in polyurethane glycolysis<sup>53</sup>.

Many scientists have studied the glycolysis of waste PU. Simioni and Modesti<sup>54</sup> examined the glycolysis products of flexible PU foams at 190°C. Their findings revealed that using ethylene glycol (EG) enabled the procedure to be carried out with a high polymer/glycol ratio (up to 4:1). The result was a polyphasic product. The end product of the research satisfied the primary requirements for a material for widespread usage in the preparation of reaction injection molding PU. Borda et al.<sup>55</sup> examined the glycolysis of flexible PU foams and elastomers in the 170-180°C temperature range. Glycols [EG, 1,2-propylene glycol, triethylene glycol, poly(ethylene glycol)] and diethanolamine were utilized as reagents. A reaction mechanism for polyurethane glycolysis was postulated in their work (**Figure 1.11**). The two-phase liquid combination polyol component was isolated and may be employed as an industrial glue.



Figure 1.11: Glycolysis reaction of polyurethane with ethylene glycol forms a peroxy acid and alcohol<sup>54</sup>.

### 1.3.3.3 Ammonolysis

Ammonia can be used as aqueous, liquid, or anhydrous ammonia in the ammonolysis process. Ammonolysis has mainly been studied for nylon and polyethylene terephthalate (PET)<sup>56,57,58</sup>. Lentz et al.<sup>59</sup> created an intriguing method for the ammonolytic cleavage of PU, which involved using supercritical ammonia for depolymerization (**Figure 1.12**). The ammonolysis reaction was conducted in a reactor of 50 mL capacity at 139 °C and 140 bar for a reaction duration of 2 hours and an extraction time of 90 minutes.

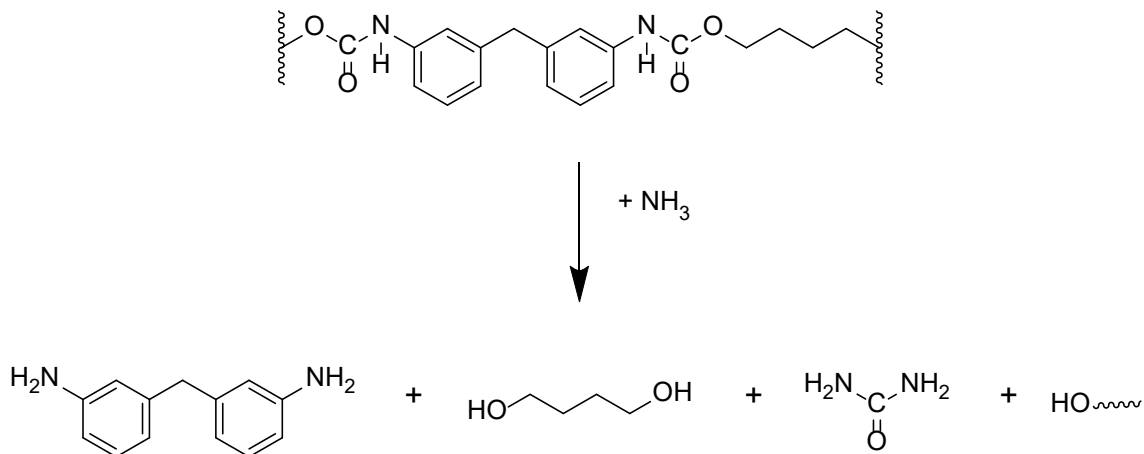


Figure 1.12: Decomposition of flexible polyurethane foam via ammonolysis using supercritical ammonia<sup>59</sup>.

Ammonolysis can also occur concurrently with other depolymerization mechanisms, such as glycolysis, hydrolysis, and alcoholysis<sup>60</sup>. However, only a few research papers on this approach for PU recycling have been published<sup>59,60,61</sup>. Sheratte published a patent on the recycling of PUFs via ammonolysis, highlighting two major stages of decomposition<sup>61</sup>. In the first stage, simultaneous glycolysis and ammonolysis employing ethylene glycol and ammonium hydroxide produced a polyol mixture with amines that were either phase-separated or processed further. The substance was then reacted with ammonia in the second stage.

Ammonolysis using ammonium hydroxide to depolymerize PUFs is the least investigated decomposition method<sup>60</sup>. It can be used alone or in conjunction with other depolymerization techniques. Because the subject has received less attention, there is still room for future modification and enhancement of the processes to increase the conversion of the reaction and the quality of the recycled product.

#### 1.3.3.4 Predicted Decomposition Mechanisms

FPUF decomposition in aqueous ammonium hydroxide can occur via a combination of ammonolysis and hydrolysis (**Figure 1.13**). The electronegativity of nitrogen is 3.04, while that of oxygen is 3.44<sup>62</sup>. Due to the lower electronegativity, the lone pair of electrons in nitrogen is loosely bound to the atom<sup>63</sup>. Thus,  $\text{NH}_3$  will act as a better nucleophile than the hydroxyl ion, leading to the ammonolysis of the carbonyl carbon in the urethane linkage before hydrolysis. FPUF undergoes ammonolysis in the first step to generate two carboxamide intermediates and the diamide ion of the diamine used to produce the initial diisocyanate monomer (**Figure 1.13**). These intermediates then decompose to produce a mixture of polyols along with the precursor diamine of the original diisocyanate monomer used to make the FPUF and carbamic acid. FPUF can also react with ammonium hydroxide via a base-catalyzed

hydrolysis mechanism to form a mixture of carboxylic acids and the diamine compound used to make the diisocyanate monomer (**Figure 1.14**).

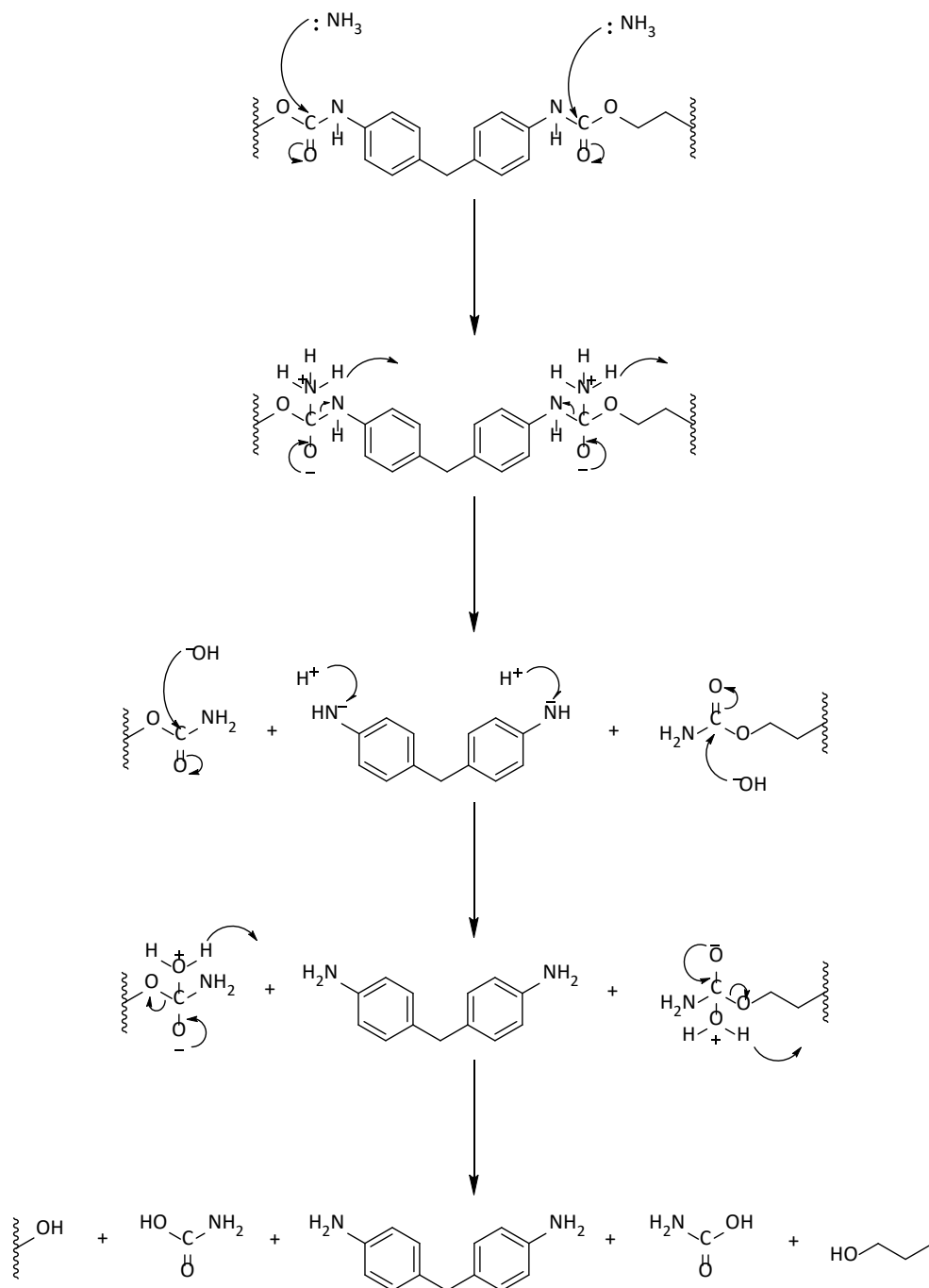


Figure 1.13: Decomposition mechanism of flexible polyurethane foam (FPUF) via combined ammonolysis and hydrolysis to form carbamic acid, 4,4'-methylenediphenyldiamine (MDA), and a polyol mixture.



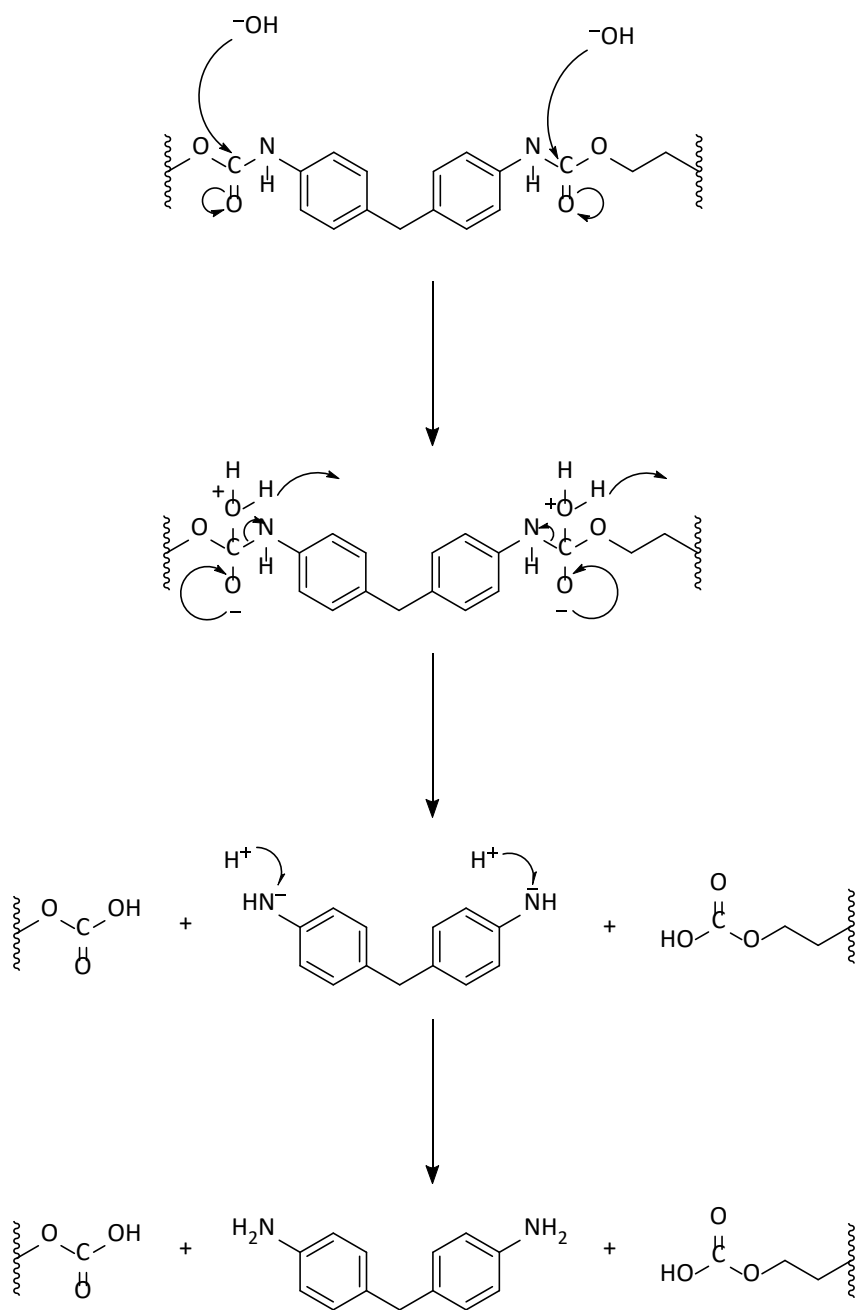


Figure 1.14: Base-catalyzed hydrolysis mechanism of flexible polyurethane foam (FPUF) to form a mixture of carboxylic acids and 4,4'-methylenediphenyldiamine (MDA).

## 1.4 Microbial Upscaling

As discussed above, PUF can be chemically degraded using ammonia to obtain a wide variety of diamines and diols depending on the monomers used during production. At the most basic level, microbes require C, H, O, N, S, P, K, Mg, Fe, Ca, Mn, and traces of Zn, Co, Cu, and Mo<sup>64</sup>, all of which, except C, can be provided by minimal media<sup>65</sup>. Pure bacterial cultures require particular carbon sources for growth. For instance, *Corynebacterium*, *Arthrobacter*, *Acinetobacter*, *Alcaligenes*, *Alkanivorax*, and *Pseudomonas* were shown to be capable of using cyclohexane carboxylic acid (CHCA) as a carbon source for growth<sup>66,67,68</sup>. Members of the genus *Rhodococcus* were recently identified from oil sands process-affected waters (OSPW) microbial communities, and early evidence of their ability to break down naphthenic acids (NAs) was provided<sup>69</sup>.

A microbial consortium enables bacteria to utilize a diverse range of carbon sources<sup>70</sup>. It gives bacteria resistance to environmental stresses. A consortium of microbes may execute complicated activities that a single organism cannot<sup>71</sup>. Using microbial consortia instead of pure microbial species is the best option to deal with the issue of using a specific complex carbon source for growth<sup>72</sup>. Additionally, microbial consortia are more flexible and stable within the growing environment. They can provide an appropriate catalytic climate for each enzyme required by the biodegradation pathway, making them preferable to isolated bacteria for degrading complex chemicals<sup>73</sup>. Complex substances, such as plastics, petroleum, antibiotics, azo dyes, and some contaminants found in sewage, can be broken down by microbial consortia<sup>73</sup>.

Typically used monomers for producing PUF include 1,2-propanediol (PDO), 1,4-butanediol (BDO), polypropylene glycol (PPG), toluene diisocyanate (TDI), and methylene diisocyanate (MDI)<sup>74</sup>. Microbes from the genus *Pseudomonas* are promising biodegradation agents for synthetic plastic waste, such as PUF<sup>75</sup>. *Pseudomonas putida* KT2440 strains have been designed to use ethylene glycol (EG) and 1,4-butanediol (BDO) as carbon sources<sup>76</sup>. A unique strain, *Pseudomonas* sp. TDA1 was recently found to use 2,4-toluenediamine (TDA), a frequent precursor of TDI, for PUF production<sup>77</sup>. Moreover, *Lactobacillus diolivorans*, a recently identified and characterized microbe, is capable of using 1,2-propanediol for its metabolism<sup>78</sup>.

## 1.5 Project Objectives

This project aimed to achieve the highest possible solubilization of flexible polyurethane foam (FPUF) in ammonium hydroxide and use the final liquid as a carbon source for microbial upscaling without adding any external carbon (**Figure 1.15**). FPUF solubilization for a temperature range of 140-200°C with intervals of 20°C was monitored at residence times of 30 minutes and 60 minutes. The chemical composition of the decomposed PUF products was determined using FTIR and NMR

spectroscopy. Growth curves were created using the generated media to investigate the growth of microbial consortia from Calumet, MI, and the straits of Mackinac. Additionally, microbial pellets were collected from the inoculated media at the beginning and end of the incubation period. Ultra-pure DNA was extracted from the collected pellets, and a library with equal volumes was pooled. DNA sequencing was conducted to determine the taxa present at the beginning of the incubation period and after 120 hours, along with their relative abundances. A toxic aromatic diamine present in the generated liquid was found to inhibit microbial growth over the course of the experiments.

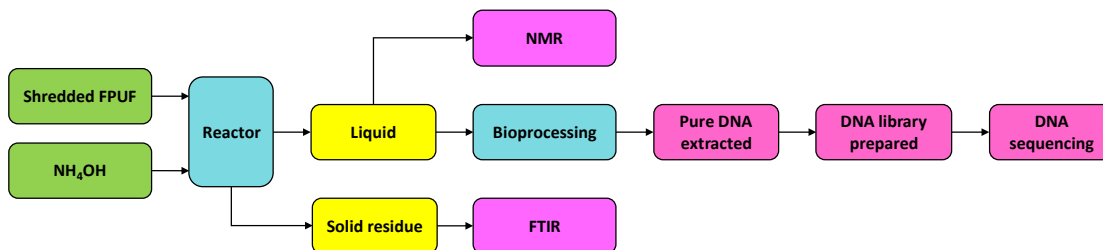


Figure 1.15: Process flowchart of the experimental process.

## 2 Materials and Methods

### 2.1 Materials

Flexible polyurethane foam (FPUF) was purchased from Amazon (Foamma F-6-2472H) along with a commercial paper shredder (Amazon Basics). Ammonium hydroxide (Sigma Aldrich, 30% w/w, CAS 1336-21-6) was diluted to 5%, 10%, 15%, and 16% w/w for experimental purposes. Liquid nitrogen (MTU ChemStores 20900), Bushnell Haas Broth (VWR), 2,4-diaminotoluene (Sigma Aldrich, 98%, CAS 95-80-7), 4,4'-diaminophenylmethane (Sigma Aldrich,  $\geq 97\%$ , CAS 101-77-0), polypropylene glycol 1000 (ThermoFisher Scientific, CAS 25322-69-4), 1,2-propanediol (Chem-Impex,  $\geq 99.5\%$ , CAS 57-55-6) and 1,4-butanediol (Sigma Aldrich, 99%, CAS 110-63-4) were used as received. Quick DNA fungal/bacterial miniprep kit (Zymo Research D6005), Quick-16S plus NGS library prep kit V3-V4 (Zymo Research D6420-PS1), and MiSeq reagent kit v3 (Illumina MS-102-3003) were used as received for DNA analysis.

### 2.2 Methods

#### 2.2.1 Preparation of FPUF

The FPUF slab purchased was cut down into manageable pieces of 25 cm  $\times$  25 cm  $\times$  25 cm and fed to the paper shredder to obtain cubical FPUF pieces of approximately 1 cm  $\times$  1 cm  $\times$  1 cm (**Figure 2.1**). The acquired particles were subjected to a Milty Zerostat 3 Anti-Static Gun to make loading the FPUF into the reactor easier. Twenty grams of FPUF was also cut into rectangular pieces of size 25 cm  $\times$  1 cm  $\times$  1 cm using scissors, dipped into liquid nitrogen using tongs and cryogenic gloves, and blended into a fine powder using a Waring Commercial laboratory blender (Model no. 31BL40).



Figure 2.1: Flexible polyurethane foam (FPUF) shredded using a paper shredder.

### 2.2.2 Thermogravimetric Analysis

Thermogravimetric analysis of the polyurethane sample was conducted by loading 8.49 mg of cryo-milled FPUF powder (**Figure 2.2**) onto the pan of a Q500 (TA instruments) thermal analyzer. The sample gas purge was set to 60 mL/minute for nitrogen and 40 mL/min for air. A heating rate of 10°C/min till a temperature of 800°C was set for the equipment. The thermal decomposition temperature of the FPUF sample was visually determined from the TGA scan.



Figure 2.2: Cryo-milled flexible polyurethane foam (FPUF) used for thermogravimetric analysis.

### 2.2.3 FPUF Decomposition in Batch Reactor

A small, custom batch reactor was assembled using a cylindrical stainless steel body (3/4 inch sanitary tubing), reactor head, a stainless steel plug, gaskets, and metal

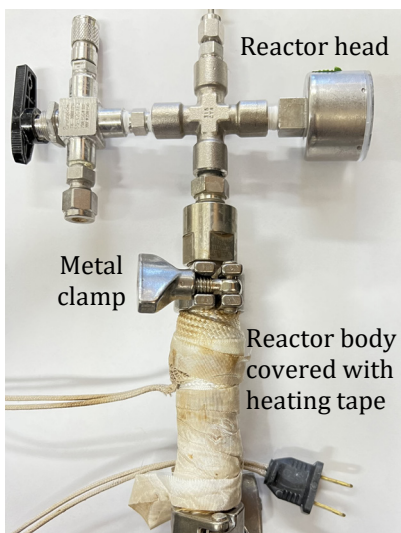


Figure 2.3: Batch reactor assembly with reactor head attached to the reactor body using metal clamps. The reactor body is covered with heating tape.

sanitary clamps (**Figure 2.3**). The total volume of the assembled reactor was 13.5 mL. Shredded FPUF pieces were weighed and loaded into the reactor with 16% w/w ammonium hydroxide at a solids loading of 62.5 g FPUF/L NH<sub>4</sub>OH (0.5 g FPUF with 8 mL NH<sub>4</sub>OH), and the reactor was placed in the upright position using a ring stand with clamps. The reactor body was covered with heating tape and connected to a voltage controller. A temperature monitor was plugged into the thermocouple that extended into the body of the reactor.

The temperature was controlled manually using a voltage controller. Once the desired reactor temperature reached -5°C of the setpoint, a timer was started to initiate the residence time. During the residence time, the temperature control was adjusted to maintain a temperature within ± 5°C of the desired setpoint.

Immediately after the residence time was completed, the voltage controller was turned off, and the reactor was cooled down to 50°C using cold air. The reactor was vented by turning the three-way valve on its head and then disassembled. The contents in the reactor were scraped out using a spatula and vacuum filtered using a Whatman grade 42 ashless filter paper (42.5 mm diameter, 2.5 µm). The liquid product was filtered again using polytetrafluoroethylene (PTFE) syringe filters (0.22 µm) and stored in glass vials for later use and analysis. The solid residue on the filter paper was placed in a drying oven at 50°C for 12 hours to remove any remaining moisture. The mass of the solid residue was recorded after moisture removal to calculate the percent solubilization as,

$$\text{Percent Solubilization} = \frac{\text{Mass of FPUF loaded} - (\text{Mass after drying} - \text{Mass of filter paper})}{\text{Mass of FPUF loaded}} \times 100\%$$

Equation 1: Percent solubilization of FPUF in NH<sub>4</sub>OH is calculated from the mass of FPUF loaded and mass of FPUF after drying.

## 2.2.4 FPUF Decomposition in a Continuous Stirred-Tank Reactor

The shredded FPUF sample was weighed and loaded into a continuous stirred-tank reactor (Parr Instrument Company, series 4560 mini benchtop reactor, 600 mL) along with 16% w/w ammonium hydroxide to maintain a solids loading of 6.25% (0.5 g FPUF in 8 mL NH<sub>4</sub>OH). The reactor body was aligned with the head, and the clamp was shut. The thermocouple was plugged into the reactor head, and the heating jacket slid onto the body. The main power supply of the reactor was then turned on. The temperature was set to the desired value using the control module of the Parr reactor, and the heater was switched on. The stirrer was then switched on and set to 60 RPM. A stopwatch was then set for the residence time to be tested. Once the reaction ran for the set residence time, the stirrer and heater were switched off. The heating jacket was removed from the reactor body while wearing heat-resistant gloves, and the main power supply switch of the system was turned off. The reactor was cooled down to 50°C using cold air.

The reactor contents were scraped out using a spatula and vacuum filtered using a Whatman grade 42 ashless filter paper (42.5 mm diameter, 2.5  $\mu\text{m}$ ). The solid residue left behind on the filter paper was oven dried at 50°C for 12 hours to eliminate all moisture. Once devoid of moisture, the solid residue was weighed to calculate the percent solubilization and then stored for analysis. The liquid product was filtered a second time using PTFE syringe filters (0.22  $\mu\text{m}$ ) to remove any remaining solid particles and stored in glass vials for later use and analysis. The generated liquid media was neutralized from a pH of 9.8 to around 6.8 using 85%  $\text{H}_3\text{PO}_4$  for microbial upcycling.

### **2.2.5 FTIR and NMR Scans**

The solid residue from the reaction was analyzed using an FTIR (Shimadzu, IR tracer 1000). The sample holder was cleaned using 90% ethanol before placing the sample to remove any impurities. The arm of the equipment was lowered, and a background scan was run to account for possible interference from the surrounding air. The FTIR was set to take 10 scans of the sample. The percent transmission was obtained at a resolution of 4  $\text{cm}^{-1}$  from a wavenumber of 400  $\text{cm}^{-1}$  to 4000  $\text{cm}^{-1}$ . The scan was analyzed using LabSolutions IR (Shimadzu) to identify all relevant peaks. The peaks were compared to a spectral repository (Wiley, SpectraBase) to determine the composition of the solid residue.

$^{13}\text{C}$  NMR analysis of the liquid product was conducted using a Bruker Ascend 500 NMR spectrophotometer. Two hundred microliters of the liquid product was diluted with 600  $\mu\text{L}$  of dimethyl sulfoxide- $\text{d}_6$  (Sigma Aldrich, 99.9 atom % D) in an NMR tube. Sixty-four scans were run with a proton lock (for  $^1\text{H}$  spectra) and a C13 lock (for  $^{13}\text{C}$  spectra) at a frequency of 20 Hz. The software used for the runs was Topspin (Bruker). The NMR sample tube was placed on the autosampler of the NMR spectrophotometer and loaded into the instrument. The sample was tuned, and a lock was performed using the software, followed by phase adjustment and shimming. The receiver gain was then adjusted, and the acquisition was begun. Post-processing of the obtained scan was done to pick peaks and integrate the peak areas. The final data was analyzed using SpectraBase (Wiley) and the NMR prediction function in ChemDraw (PerkinElmer) to determine the compounds present in the liquid product.

### **2.2.6 Microbial Upcycling with FPUF Liquid**

Three different microbial consortia were obtained from the Department of Biological Sciences at Michigan Technological University. These were Laura 1 (LS1\_Calumet), Laura 2 (LS2\_Calumet) and Emma 2 (EB2\_Mackinac). Calumet, Michigan (Coordinates 47.211, 88.553) agricultural compost was used to create the

Laura 1 and Laura 2 cultures. At the same time, Emma 2 is a low-diversity microbial community created from acquired from sediments collected from the straits of Mackinac island (Coordinates 46.532, -88.141).

Bushnell Haas media was prepared by adding 3.27 g of Bushnell Haas media to 1 L of distilled water. After adding disodium terephthalate as the carbon source for the consortia in Bushnell Haas media, the mixture was autoclaved at 121°C for 20 minutes. The cultures were incubated in 500 mL Erlenmeyer flasks at 30°C in a shaking incubator at 200 rpm to grow the seed culture. Cultures were maintained at 250 mL, and 100 mL of spent culture was replenished with 400 mL of fresh 10 g/L disodium terephthalate in Bushnell Haas medium every 7 days.

Microbial media was prepared by adding 50 mL of autoclaved Bushnell Haas media, and 2 mL of the generated neutralized FPUF liquid with the highest solubilization percentage to 250 mL Erlenmeyer flasks. The media was inoculated with all three microbial consortia in triplicate to a target initial optical density (OD<sub>600</sub>) of 0.3.

The flasks were placed in a shaking incubator at 30°C at 200 rpm for 120 hours. During incubation, the optical density of the sample at 600 nm was measured at periodic intervals to monitor microbial growth. At the end of the growth period, 1 mL of the consortia media was pipetted into a 2 mL microcentrifuge tube and centrifuged at 12,000 rpm for 5 minutes. The supernatant was pipetted out, and the microbial pellets were stored in a -20°C freezer for use later. Microbial growth curves were prepared to compare the growth of different cultures in the media.

Additionally, more FPUF liquid was generated at a solids loading of 25% FPUF in 16% w/w ammonium hydroxide (5 g FPUF in 20 mL NH<sub>4</sub>OH) to observe the effect of the presence of a higher percentage of carbon source in the media. The media was prepared under the same conditions as the previous experiments. It was inoculated with all three microbial consortia in triplicates to an initial optical density (OD<sub>600</sub>) of 0.3 and incubated at 30°C for 120 hours at 200 rpm. The optical density of the samples was monitored periodically, and microbial growth curves were prepared to compare the results. Microbial pellets were collected and stored in a -20°C freezer for later use.

### **2.2.7 Microbial Upcycling with Standard Chemical Media**

Standard FPUF decomposition products, including 2,4-diaminotoluene, 4,4'-diaminophenylmethane, polypropylene glycol (1000), 1,2-propanediol, and 1,4-butanediol were added to 52 mL autoclaved Bushnell Haas media in 250 mL Erlenmeyer flasks. Calculated amounts of each chemical (**Table 2.1**) were added to maintain the same mass concentration as total carbon sources in the FPUF liquid generated from the 25% solids loading reaction from the previous experiments (8.8 g/L). It was assumed that the microbial consortia can utilize the entire amount of carbon present in the FPUF liquid media. The flasks were incubated at 30°C in a



shaking incubator at 200 rpm for 120 hours, during which the optical density at 600 nm was measured periodically to monitor microbial growth. At the end of the growth period, 1 mL of liquid was pipetted into a 2 mL microcentrifuge tube and centrifuged at 12,000 rpm for 5 minutes to gather microbial pellets at the bottom of the tube. The supernatant was removed, and the microbial pellets were stored in a -20°C freezer for DNA analysis.

Table 2.1: Mass of standard chemicals added to prepare media for microbial upcycling.

Chemical	Mass added (g)
2,4-diaminotoluene	0.5
4,4'-diaminophenylmethane	0.505
1,2-propanediol	0.492
1,4-butanediol	0.495
Polypropylene glycol (1000)	0.476

## 2.2.8 DNA Analysis

The collected microbial pellets were resuspended in 1 mL of distilled water and processed using a Zymo Quick DNA fungal/bacterial miniprep kit as per the instruction manual in the kit to obtain ultra-pure DNA. Zymo Quick-16S plus NGS library prep kit V3-V4 was used for library preparation and cleanup. Each DNA sample obtained was pipetted (2 µL) into the wells of a Zymo primer set 1 PCR plate (columns 1 through 6, rows A through H, excluding wells G6 and H6). Positive and negative controls were included in wells G12 and H12 of the PCR plate. All PCR reactions were pipette mixed, and an adhesive PCR plate seal was applied to the plate. The plate was centrifuged in a microplate centrifuge (Fisherbrand) at 1200 g for 1 minute. The PCR plate was then run in a thermocycler (Eppendorf, Mastercycler Pro S vapo protect) using the program shown in **Table 2.1**. Once the program was complete, the plate was centrifuged in a microplate centrifuge (Fisherbrand) at 1000 g for 30 seconds to collect condensation in the wells.

Table 2.2: Real-time thermocycler program for PCR plate reactions.

Temperature	Time
95°C	10 min
95°C	30 sec
55°C	30 sec
72°C	3 min
Plate read	-
4°C	Hold

Agarose gel was then prepared by mixing 0.5 g of agarose (Fisher BioReagents, CAS 9012-36-6) with 50 mL 1X TAE buffer in a 250 mL Erlenmeyer flask. The contents of the flask were microwaved until slight bubbling was observed. Two microliters of SYBR safe DNA gel stain was then added to the gel and mixed before pouring out the

gel into a gel electrophoresis system (Thermo Scientific, EasyCast B1). Two combs were placed in the gel to make wells and left to settle for 20 minutes (until the gel turned opaque). Three microliters of 6 random DNA samples were mixed with 2  $\mu\text{L}$  of bromophenol blue dye and injected into the wells with positive and negative PCR controls and a ladder. The entire setup was run at 75 V for 45 minutes. The final gel was observed under a BioDoc-It UVP imaging system to validate the success of PCR amplification.

Equal volumes ( $\mu\text{L}$ ) of PCR products from each well of the PCR plate were pooled into a 1.5 mL microcentrifuge tube. The pooled liquid was subjected to final library cleanup per section 3 of the instruction manual provided by the manufacturer. The final library was diluted and quantified using a fluorescence-based method (Qubit dsDNA HS Assay Kit) to an average of 8.89 ng/ $\mu\text{L}$  DNA.

The pooled DNA library was sequenced using an Illumina MiSeq reagent kit v3 (600 cycles). All reagents in the kit were thawed out at room temperature. The collected DNA library and PhiX were diluted to 4 pM using the HT1 buffer provided in the sequencing kit and denatured using freshly prepared 0.2 N NaOH. Diluted and denatured PhiX and DNA library were mixed at a ratio of 1:9 to obtain a final volume of 600  $\mu\text{L}$ . This liquid mixture was denatured on a heat block at 96°C. The flow cell from the kit was washed using ultrapure water, followed by 70% ethanol, blotted dry using Kim wipes, and inserted into the Illumina MiSeq system. The sample was loaded onto the reagent cartridge and placed in the sequencer.

The FASTQ file, a text-based file that stores DNA sequences, was obtained from the MiSeq after the sequencing run. This file was imported into Rstudio, cleaned using the tidyverse package, and converted into a .csv file. A DNA sequence table was then generated, and taxonomy was assigned to this table after removing chimeras. The phyloseq package was then used to generate cleaned sequence and taxa tables, and both tables were combined into one single phyloseq object. Eukaryotes, chloroplast, and mitochondria were filtered out from the generated object, and the final data was normalized for analysis. The reproducible data was then filtered out to make a genus taxa and species classification plot.

## 3 Results and Discussion

### 3.1 Thermogravimetric Analysis

Based on the thermogravimetric scan of FPUF, the thermal decomposition temperature of the sample can be estimated<sup>79</sup>. Due to the breakdown of the urethane bonding, the first decomposition step started around 210°C in FPUF (**Figure 3.1**). The second stage of decomposition started at about 400°C due to the breakdown of the hard isocyanate segments that give the foam structural strength<sup>79</sup>. The sample weight inside the TA Q500 thermogravimetric analyzer started deviating from the baseline at 210°C. Thus, to avoid thermal decomposition of FPUF, the reaction temperature must be maintained below 210°C.

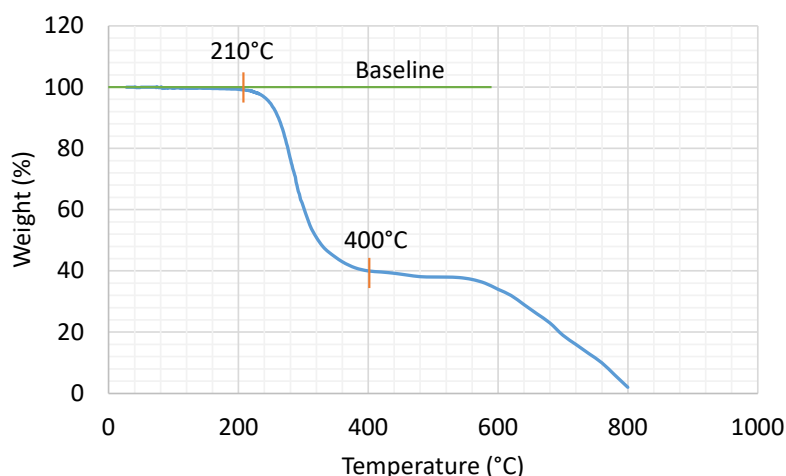


Figure 3.1: Thermogravimetric scan of flexible polyurethane foam (FPUF) shows a 2-step thermal decomposition. The sample starts decomposing at 210°C followed by a second decline in the weight percent at 400°C.

### 3.2 Solubilization of FPUF in $\text{NH}_4\text{OH}$

#### 3.2.1 Batch Reactor

The solubilization of FPUF in 16% (w/w)  $\text{NH}_4\text{OH}$  at a weight percent solids loading of 6.25% in a self-assembled small batch reactor of 13.5 mL volume was analyzed in triplicate for a residence time of 30 and 60 minutes at different temperatures. Temperatures tested were kept below 210°C to prevent the thermal decomposition of FPUF. The average solubilization was found to increase as the temperature increased (**Figure 3.2**). Raising the residence time of the reaction time to 60 minutes also led to an increase in the average solubilization. However, maximum

solubilization of only 53% was achieved in the batch reactor at 200°C, 200 psi for a residence time of 60 minutes at a solids loading of 62.5 g FPUF/L 16% NH<sub>4</sub>OH. Reactants were introduced into the system at a macro-scale. The pure reactants must be homogenized at the molecular level for molecules to collide and react<sup>80</sup>. Hence, improper mixing was the limiting factor for solubilization in a batch reactor.

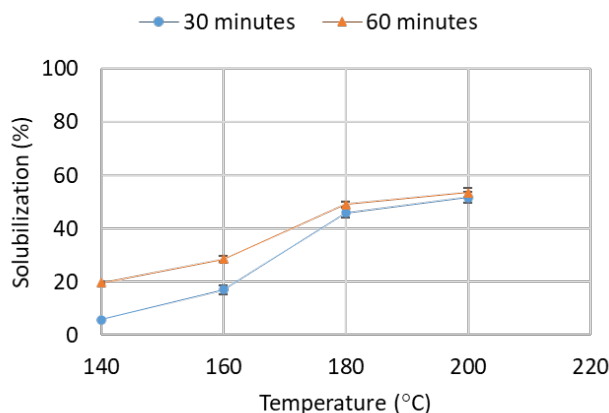


Figure 3.2: Flexible polyurethane foam (FPUF) solubilization in a custom batch reactor increased with temperature and time to a maximum of 53% for 62.5 g FPUF/L 16% NH<sub>4</sub>OH. Error bars represent the average  $\pm$  standard deviation (n=3).

### 3.2.2 Continuously Stirred-Tank Reactor

Significantly better results were observed when FPUF was reacted at the same conditions in a Parr reactor with stirring (60 rpm). At a residence time of 30 minutes, the percent solubilization increased gradually with temperature and time (**Figure 3.3**). The trend for a residence time of 60 minutes was similar. It was noted that the solubilization did not go above 95% when the residence time was bumped up to 60 minutes. Due to the generation of insoluble by-products, achieving a higher percent solubilization was difficult. Thus, the ideal reaction conditions for the highest possible solubilization of FPUF in a continuously-stirred tank reactor (Parr reactor) was determined to be at 30 minutes, 200°C, and 200 psi at 60 rpm for a solids loading of 62.5 g FPUF/L 16% NH<sub>4</sub>OH.

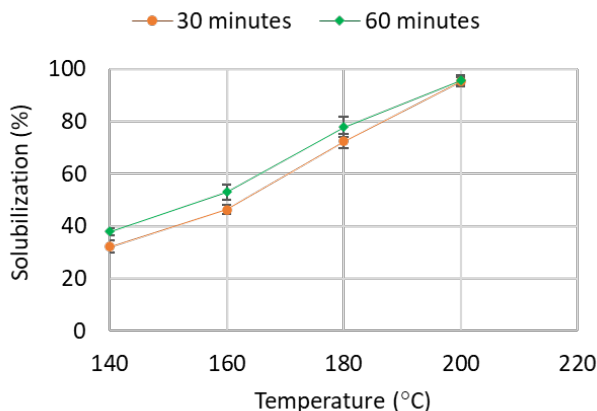


Figure 3.3: Flexible polyurethane foam (FPUF) solubilization in a Parr reactor increased with temperature and time to a maximum of 95% for 62.5 g FPUF/L 16%  $\text{NH}_4\text{OH}$ . Error bars represent the average  $\pm$  standard deviation ( $n=3$ ).

### 3.2.3 Effect of Higher Solids Loading of FPUF

FPUF decomposition reactions were conducted at 200°C, 30 minutes, and 200 psi in a Parr reactor at 60 rpm for solids loading of 10, 15, 20, 25, and 30 weight percent in triplicates. It was found that the percent solubilization remained above 90% until reaching a solids loading of 25% PUF in 16% w/w  $\text{NH}_4\text{OH}$  (250 g PUF/L 16%  $\text{NH}_4\text{OH}$ ). However, at 30% solids loading, the large amount of loaded solids led to poor mixing of the reactants, which resulted in an incomplete reaction, thus reducing the solubilization to 75.5%<sup>81</sup> (**Figure 3.4**). Five grams of shredded FPUF was added with 16.67 mL of 16% (w/w)  $\text{NH}_4\text{OH}$  for the 30% solids loading reaction.

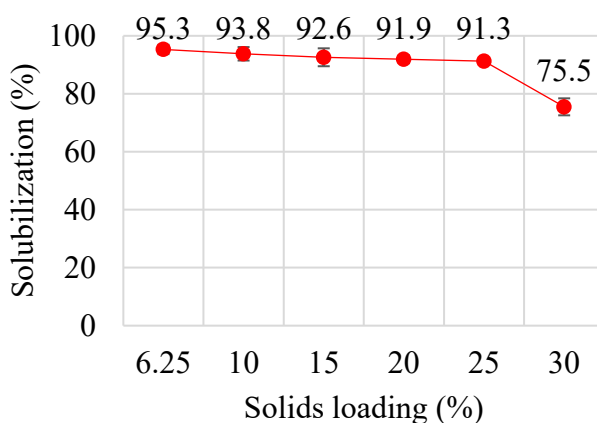


Figure 3.4: Percent of FPUF solubilized in ammonium hydroxide remains above 90% until a solids loading of 30% FPUF. Error bars represent average  $\pm$  standard deviation.

### 3.3 FTIR and NMR Analysis

FPUF decomposed into a dark solid residue along with a brownish liquid (**Figure 3.5, Figure 3.7**) upon reaction with 16% w/w  $\text{NH}_4\text{OH}$  at  $200^\circ\text{C}$ , 200 psi at a residence time of 30 minutes. The solid residue, upon drying, lost most of its weight and yielded black particles (**Figure 3.5**). The peaks in the functional group region of the FTIR spectroscopy of the obtained particles in air at room temperature were analyzed (**Figure 3.6**).

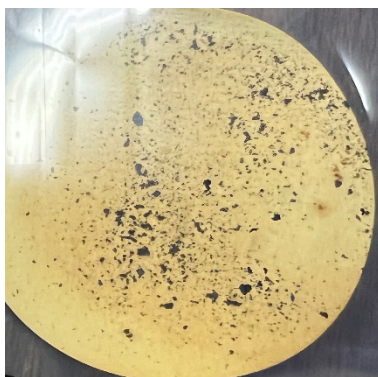


Figure 3.5: Residual solid particles from FPUF ammonolysis after filtration and oven drying at  $55^\circ\text{C}$ . Reaction conditions:  $200^\circ\text{C}$ , 200 psi, 30 minutes for 25% solids loading (g FPUF per mL  $\text{NH}_4\text{OH}$ ) at 60 rpm.

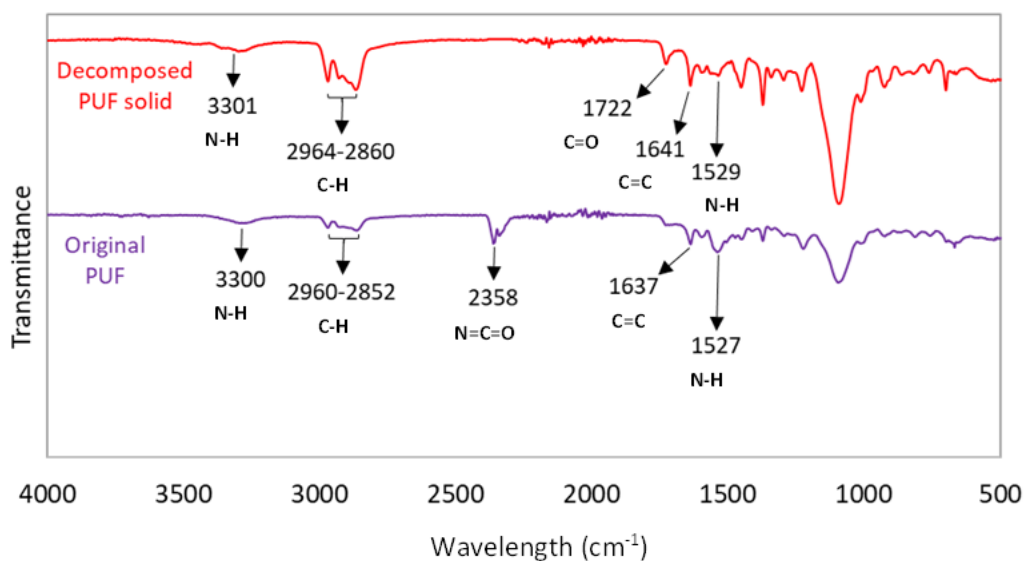


Figure 3.6: FTIR spectra of original FPUF sample and decomposed solid obtained after product filtration shows the decomposition of urethane bonds after the reaction.

The FTIR spectra of solids obtained at all solids loading percentages tested were the same. This indicated that the product obtained under different conditions were the same; however, the amount of dissolved carbon source differed. The broad band at  $3301\text{ cm}^{-1}$  and  $3300\text{ cm}^{-1}$  represent the stretching vibrations of N-H in the decomposed solid product and original FPUF sample, respectively. At the same time, the in-plane bending vibration of N-H is confirmed by the medium-strong peaks at  $1527\text{ cm}^{-1}$  in the original sample spectra and  $1529\text{ cm}^{-1}$  in the decomposed product scan. The group of peaks between  $2964\text{ cm}^{-1}$ – $2860\text{ cm}^{-1}$  (decomposed solid) and  $2960\text{ cm}^{-1}$ – $2852\text{ cm}^{-1}$  (pre-reaction FPUF sample) is typical of the stretching vibration of C-H<sup>82</sup>. The small sharp peak at  $1641\text{ cm}^{-1}$  and  $1637\text{ cm}^{-1}$  corresponded to the C=C bondings in the benzene ring of the decomposed solid and PUF sample, respectively. The  $2358\text{ cm}^{-1}$  absorption peak in the original FPUF scan is caused by the C=O linkage of the urethane bond in the structure<sup>83</sup>. There is no urethane band in the spectra of the decomposed solid indicating that all urethane bonds present in our FPUF sample were cleaved. A new sharp adsorption peak appeared at  $1722\text{ cm}^{-1}$  in the decomposed solid product signifying the presence of C=O bonding.

A brown liquid was obtained after filtration of the FPUF decomposition reaction. This liquid was passed through syringe filters to obtain a clear reddish-brown liquid (**Figure 3.7**). The  $^{13}\text{C}$ -NMR spectra of the reddish-brown liquid diluted in DMSO was analyzed (**Figure 3.8**).

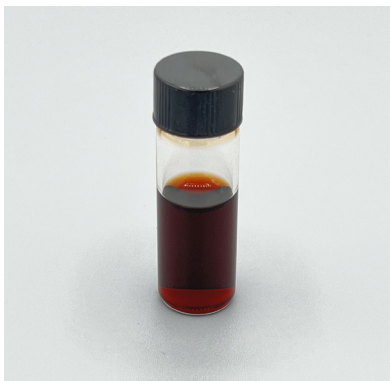


Figure 3.7: Liquid product obtained from flexible polyurethane foam (FPUF) decomposition at 25% solids loading (g FPUF/mL 16%  $\text{NH}_4\text{OH}$ ) in a Parr reactor at  $200^\circ\text{C}$ , 30 min, and 60 RPM.

Generally, the chemical shift of carbon atoms attached to an alkane chain shows up between 5-30 ppm in the  $^{13}\text{C}$ -NMR scan. The peak at 16.4 ppm represents the presence of a  $\text{CH}_3$  group at one end of the compound. Peaks between 100-155 ppm are typical of carbon environments in the benzene ring of aromatic compounds. Six peaks – 2, 3, 4, 5, 6 were found to be in the aromatic region, of which peaks 2 and 4 (**Figure 3.8**) were found to have the highest chemical shift due to the presence of an  $\text{NH}_2$  group alongside their respective carbon environments. The chemical shifts of the carbon atoms in different environments of the NMR spectra (**Table 3.1**)

indicated the presence of 2,4-toluene diamine in the liquid product. The unknown peaks at around 10 ppm (**Figure 3.8**) possibly represent the carbon atoms attached to the alkane polyol compound in the liquid product. While the 4 unknown peaks between 160-170 ppm fall in the nitrile ( $C\equiv N$ ) and oxime ( $>C=NOH$ ) region. These peaks probably correspond to the carbon environments in the by-products produced by the decomposition reaction.

Table 3.1:  $^{13}C$  NMR chemical shift and corresponding carbon environment.

Chemical shift (ppm)	Carbon environment number
16.4	1
103	3
106.2	5
112.9	7
131	6
145.4	4
146	2

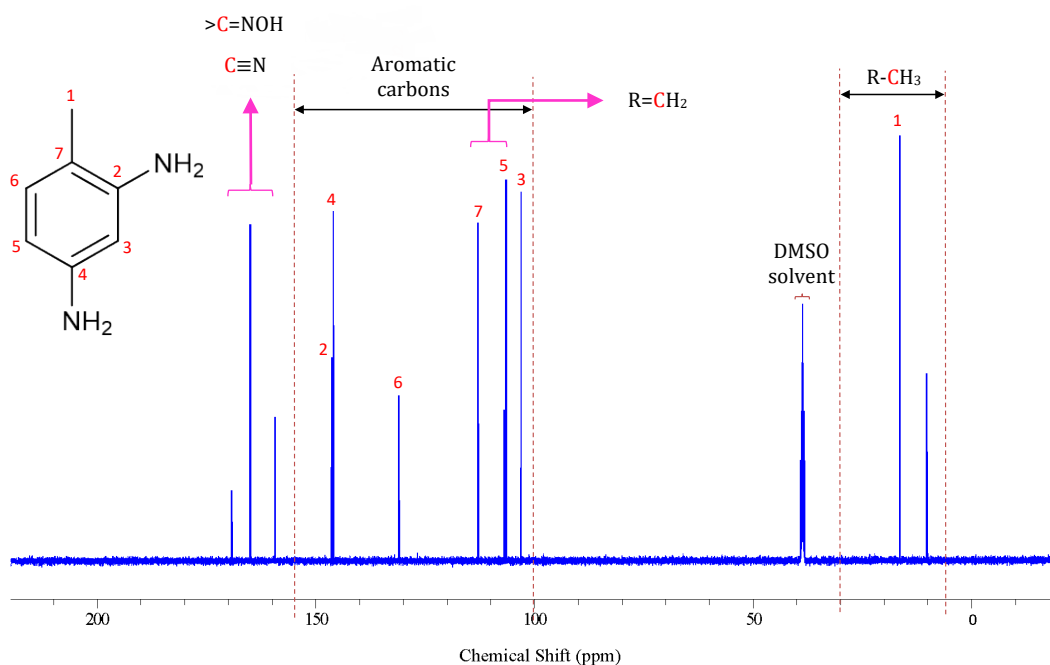


Figure 3.8:  $^{13}C$  NMR analysis of the obtained liquid product and predicted carbon source, 2,4-toluenediamine for microbial growth.

### 3.4 Upcycling of Microbial Consortia

After an incubation period of 120 hours, Laura 1 and Laura 2 microbial consortia were found to be least adaptive to FPUF liquid with a pH of 6.81 (**Figure 3.9(a)**). Emma 2 showed slightly better growth results, with a maximum  $OD_{600}$  of 0.34 from a starting  $OD_{600}$  of 0.3. This low growth was possibly because of a low carbon



content of 2.3 g/L carbon in the PUF media obtained when 62.5 g PUF was loaded per L  $\text{NH}_4\text{OH}$ . Although the microbial growth improved marginally when the FPUF liquid product with 8.8 g/L carbon was used, the  $\text{OD}_{600}$  was still  $< 0.4$  (**Figure 3.9(b)**). The Emma 2 consortia could not cross the threshold of an  $\text{OD}_{600}$  of 0.36, and Laura 1 and Laura 2 showed no growth after an incubation period of 120 hours at a pH of 6.75.

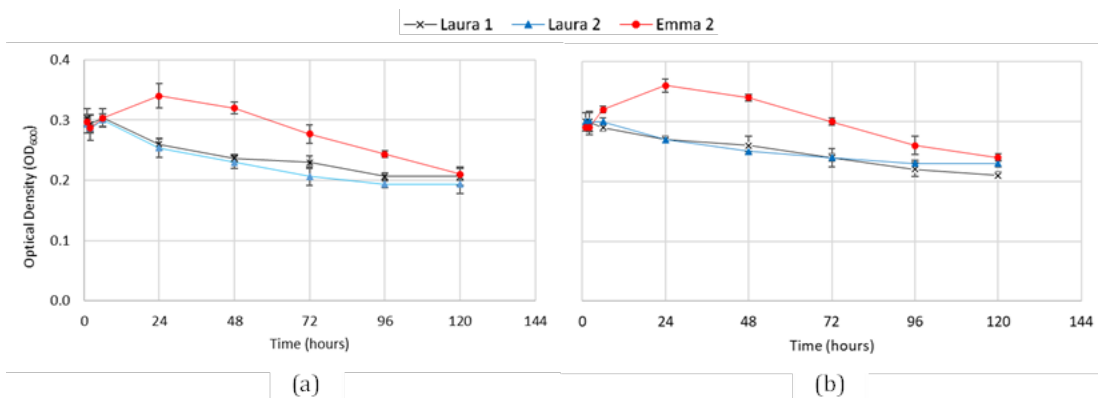


Figure 3.9: Optical density ( $\text{OD}_{600}$ ) found to be lower for microbial consortia (Laura 1, Laura 2, and Emma 2) in Bushnell Haas media with FPUF concentrations of (a) 2.3 g /L and (b) 8.8 g/L. Error bars represent average  $\pm$  standard deviation ( $n=3$ ).

Upon using aromatic diamines and diols (possible products of FPUF deconstruction) (**Figure 3.10**) as a carbon source for microbial consortia, it was found that microbial growth was inhibited by polypropylene glycol 1000, 2,4-toluenediamine (TDA), and 4,4'-methylenedianiline (MDA) (**Figure 3.11**). Polypropylene glycol (PPG) (molecular weight 1000) was possibly inaccessible by the microbial consortia due to the poor solubility of the compound or the fact that the organisms are unable to metabolize it. It was found to be immiscible in Bushnell Haas media at  $30^\circ\text{C}$ ; increasing the temperature to  $50^\circ\text{C}$  did not affect the solubility. TDA and MDA, on the other hand, were found to be toxic for all three microbial consortia used. These chemicals are carcinogens and are detrimental to the metabolism of organisms<sup>84</sup>. However, when used as the carbon source for the Emma 2 culture, the aromatic amines followed a similar pattern to the FPUF liquid, with an initial increase in growth in the first 24 hours, followed by a slow decline in  $\text{OD}_{600}$ .

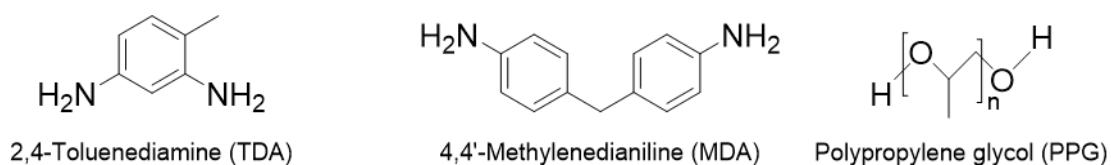


Figure 3.10: Standard chemicals 2,4-toluenediamine (TDA), 4,4'-methylenedianiline (MDA), and polypropylene glycol (PPG) used for microbial upcycling experiments.

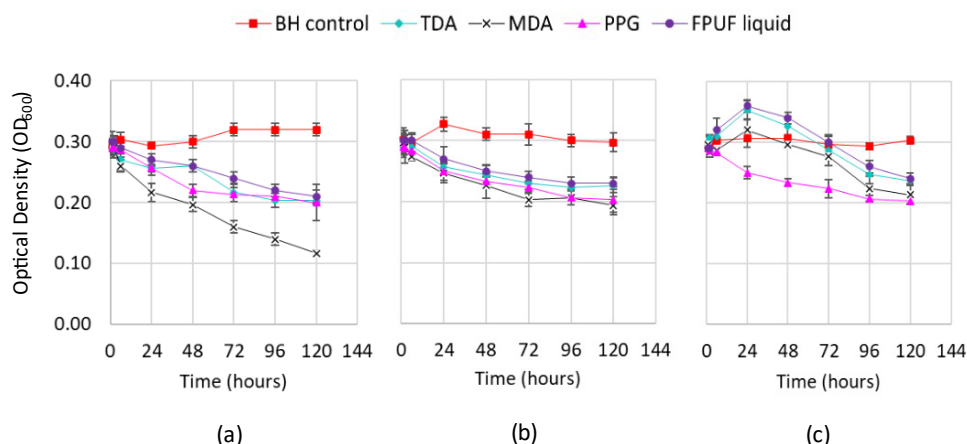


Figure 3.11: (a) Laura 1 and (b) Laura 2 cultures show no growth in FPUF media or any of the standard chemicals at a mass concentration of 8.8 g/L, while (c) Emma 2 shows slight growth in FPUF media, 2,4-toluenediamine (TDA), and 4,4'-methylenedianiline (MDA). PPG = polypropylene glycol. Error bars represent average  $\pm$  standard deviation ( $n=3$ ).

In contrast to TDA and MDA, the expected diol products, 1,2-propanediol (PDO) and 1,4-butanediol (BDO), showed impressive growth in all three microbial consortia (**Figure 3.12**). The highest  $OD_{600}$  recorded for Laura 1 consortia was 2.49 in a media containing 8.8 g/L PDO in BH media after 120 hours. Emma 2 growth in PDO was similar to that of Laura 1 at an  $OD_{600}$  of 2.6 after an incubation period of 120 hours. The Laura 2 consortia performed equally well in BDO and PDO. It was observed that after an incubation time of 120 hours,  $OD_{600}$  of Laura 2 consortia shot up to 2.79 and 2.68 in 8.8 g/L of PDO and BDO, respectively.

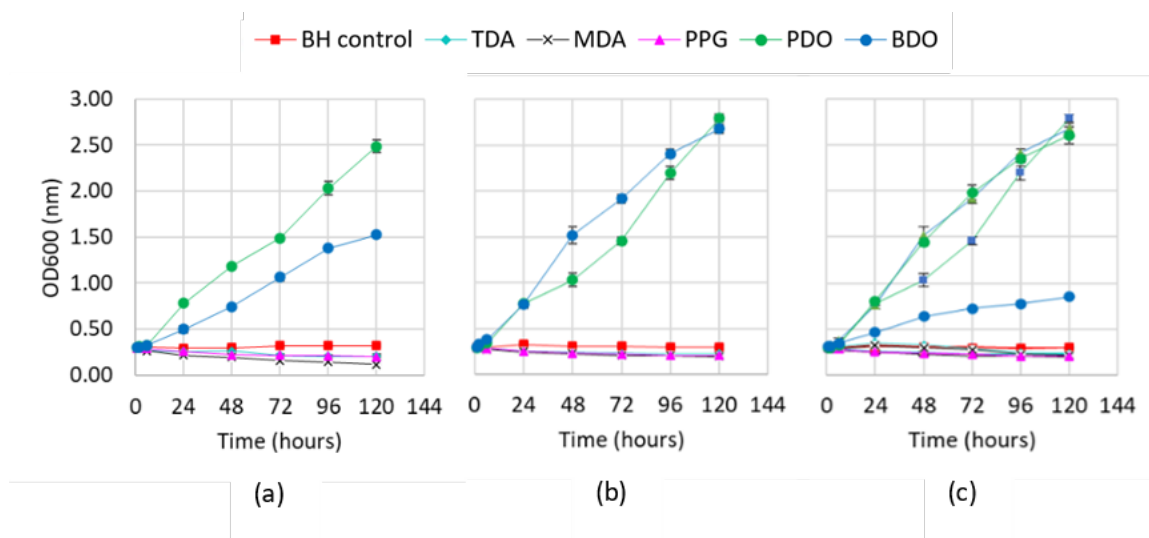


Figure 3.10: Microbial consortia (a) Laura 1, (b) Laura 2, and (c) Emma 2 show high growth in 1,2-Propanediol (PDO) and 1,4-Butanediol (BDO) as compared to other standard chemicals. All compounds were added as the sole carbon source at 8.8 g/L in BH media. TDA = 2,4-toluenediamine (TDA); MDA = 4,4'-methylenedianiline; PPG = polypropylene glycol. Error bars represent avg  $\pm$  sd (n=3).

### 3.5 Relative Abundance of Microbial Communities and Species

Comparing the genus taxa plot revealed that *Rhodococcus* sp. and *Pseudomonas* sp. were the most abundant of more than 14 genera identified in our DNA sequencing samples (**Figure 3.13**). The abundance of *Rhodococcus* after an incubation period of 120 hours in a media prepared by adding 2 mL FPUF liquid to 50 mL BH broth increased for Laura 2 and Emma 2 cultures, while it dropped significantly for Laura 1 consortia (**Figure 3.13**). The precursor standard chemical diamines of the diisocyanates used to make FPUF – TDA and MDA did not promote any microbial growth of *Rhodococcus* sp. due to their high toxicity<sup>85</sup>. The relative abundance of *Chelatococcus* sp. increased in the standard TDA and FPUF media inoculated with Laura 1 and Emma 2. Initially, the OD<sub>600</sub> of FPUF media inoculated with Emma 2 increased marginally (**Figure 3.11(c)**), indicating that *Chelatococcus* sp. may be responsible for the degradation of TDA present in the generated FPUF media.

The abundance of *Pseudomonas* was found to increase over time in media prepared using the diols used to make PUF (PDO and BDO), but they could not grow in TDA, MDA, and PPG (**Figure 3.13**)—this lack of abundance in the final liquid can be attributed to the toxicity of TDA and MDA, and the inability of *Pseudomonas* to metabolize PPG. Various species of *Pseudomonas* have been reported to be able to metabolize 1,4-butanediol<sup>86</sup> and 1,2-propanediol<sup>87</sup>. The generated FPUF media stopped certain species of the genus *Pseudomonas* present in Laura 2 and Emma 2 consortia from increasing their population.

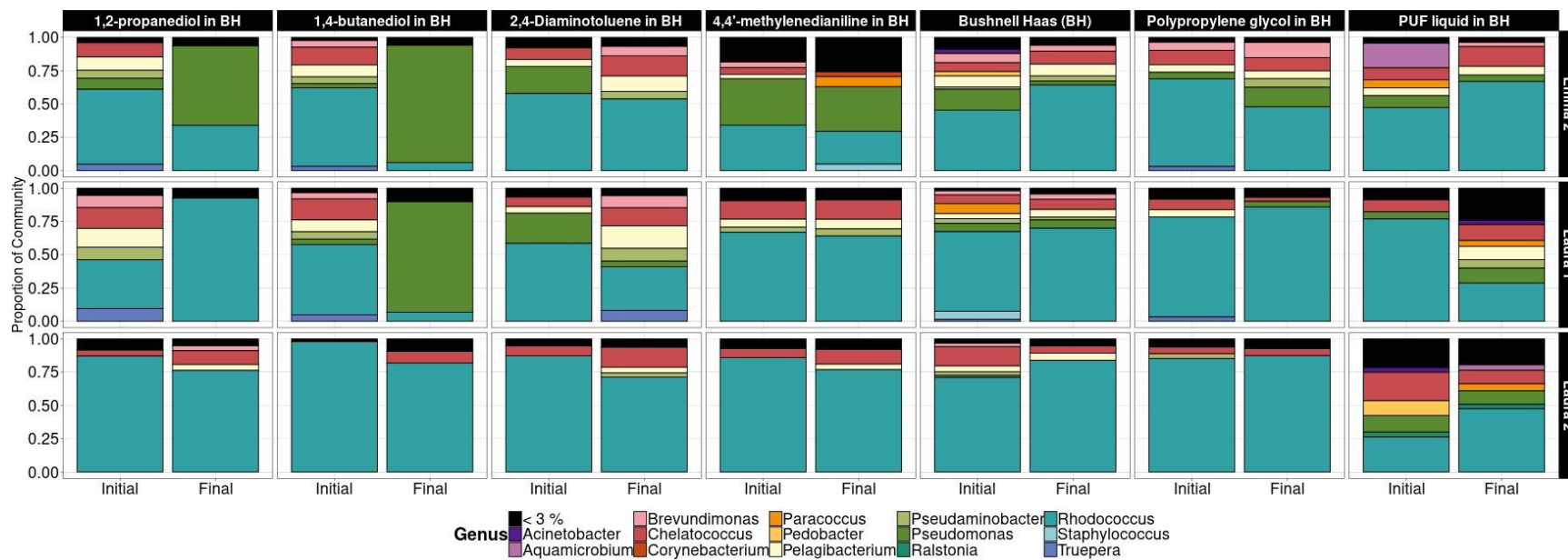


Figure 3.11: Genus taxa plot of microbial communities before and after the incubation period shows the change in relative abundance of microbial communities over time.

A species classification plot was also generated; over 13 different species of bacteria were identified (**Figure 3.14**). Of the 13 species, 3 identified species were *Rhodococcus* sp., and another 3 were classified as *Pseudomonas* sp.. The relative abundances of *Chelatococcus daeguensis* and *Brevudimonas diminuta* increased measurably in FPUF liquid media and TDA media inoculated with Laura 1 and Emma 2 consortia. This increase in the population of *C. daeguensis* and *B. diminuta*, combined with the initial rise in OD<sub>600</sub> of Emma 2 in FPUF media, suggests that TDA was possibly degraded by at least one of these species in FPUF liquid. Since the OD<sub>600</sub> declines rapidly afterward, it is possible that toxic byproducts are being produced during metabolism. It might also be possible that the amount of carbon in the FPUF media is not high enough for *C. daeguensis* and *B. diminuta* to grow simultaneously.

Certain strains of *Pseudomonas mendocina* are able to degrade a wide range of organic solvents, including toluene and alkanols like heptanol<sup>88</sup>. Other *Pseudomonas* species like *P. putida* KT2240 have been reported to be able to consume ethylene glycol<sup>77</sup>. The OD<sub>600</sub> of microbial consortia increased throughout the incubation period (**Figure 3.12**). As observed from the species classification plot (**Figure 3.14**), the relative abundance of *Pseudomonas mendocina* increased significantly in Laura 1 and Emma 2 cultures grown in 1,4-butanediol (BDO) and Emma 2 in 1,2-propanediol (PDO). This increase suggests that *P. mendocina* was able to metabolize BDO and PDO better than the rest of the microbial species. Additionally, *Rhodococcus aetherivorans* and *Rhodococcus pyridinivorans* present in Laura 1 and Laura 2, respectively appear able to metabolize PDO.

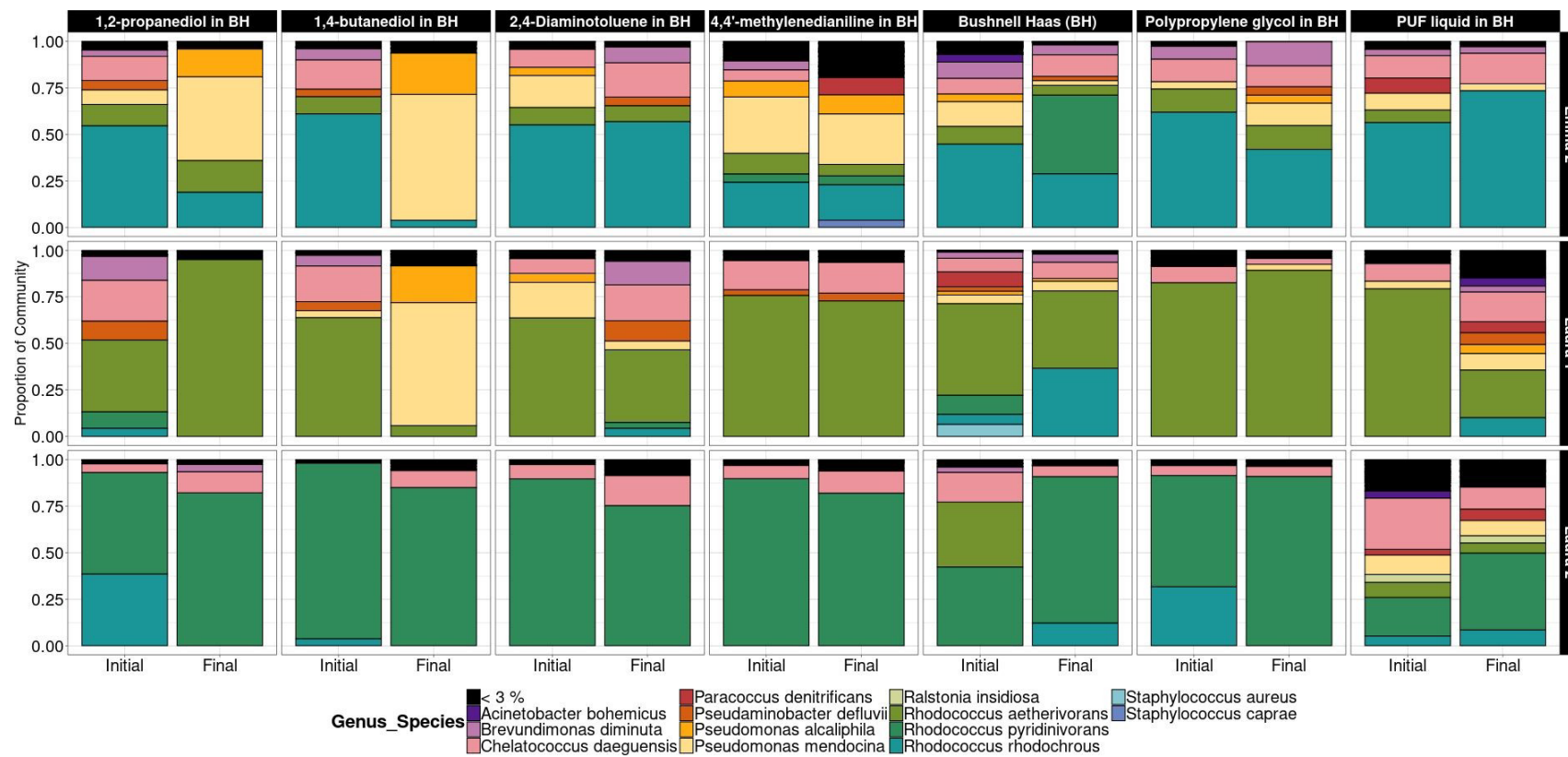


Figure 3.12: Species classification plot indicates the possible ability of *Brevundimonas diminuta* and *Chelatococcus daeguensis* present in Laura 1 and Emma 2 cultures to metabolize 2,4-toluenediamine (TDA) present in FPUF liquid media.

## 4 Conclusions and Recommendations

While we could not obtain high solubilization of FPUF in 16%  $\text{NH}_4\text{OH}$  in a batch reactor, this was not the case in a stirred tank reactor. The highest solubilization of FPUF in 16%  $\text{NH}_4\text{OH}$  obtained was 95% percent at 0.0625 g FPUF/mL  $\text{NH}_4\text{OH}$  at 200°C, 200 psi, and 60 rpm, along with a residence time of 30 minutes. Introducing an impeller into the system ensured maximum contact between all reactants and eliminated the possibility of the formation of hot spots during the reaction. The solubilization remained above 90% till a solids loading of 0.25 g FPUF/mL  $\text{NH}_4\text{OH}$ , beyond which the size of the reactor became a constraint for the reaction to yield maximum output.

FTIR and NMR spectroscopy revealed that almost all urethane bonds in FPUF were successfully cleaved by  $\text{NH}_4\text{OH}$  during the reaction leading to the formation of a liquid with TDA as one of the primary products. Bioprocessing experiments revealed that the optical density (at 600 nm) of 3 different microbial consortia (Laura 1, Laura 2, and Emma 2) inoculated with FPUF liquid decreased gradually over the course of the incubation period. Initially, this decline was attributed to the presence of 2,4-toluenediamine (TDA) due to the toxicity of this compound. Bioprocessing of the standard chemicals yielded similar optical density results as that of the FPUF media. TDA and MDA replicated the Emma 2 growth pattern seen in FPUF media, with rapid initial growth in the first 24 hours, followed by a slow decline. No growth was observed for media containing polypropylene glycol (PPG), while media containing 1,2-propanediol (PDO) and 1,4-butanediol (BDO) were able to facilitate significant microbial growth within 120 hr.

DNA sequencing of collected microbial pellets revealed that a strain of *Chelatococcus daeguensis*, *Rhodococcus pyridinovorans*, and *Rhodococcus rhodochrous* increased in relative abundance throughout the incubation period. When consortia were cultivated in media containing pure TDA and FPUF liquid, *Brevudimonas diminuta*, and *Chelatococcus daeguensis* were found to be relatively enriched. This enrichment, combined with the initial increase in OD<sub>600</sub> of microbial consortia grown in TDA and FPUF liquid media, followed by a rapid decline thereafter, suggest either generation of a toxic by-product or rapid depletion of the carbon source.

This work is important for the scientific community because achieving high solubilization of FPUF in an inexpensive solvent like  $\text{NH}_4\text{OH}$  is a crucial step toward developing new methods of recycling and upcycling waste PUFs. 2,4-toluenediamine (TDA), a raw material used to produce TDI, a vital monomer for PU production, was also identified in our FPUF liquid. Furthermore, this work identified two microbial species, *Brevudimonas diminuta*, and *Chelatococcus daeguensis*, that might be able to metabolize 2,4-toluenediamine (TDA), which is classified as a carcinogenic compound.

It is recommended that further analysis of the generated FPUF liquid should be conducted to determine whether other carbon compounds are present that may be associated with plasticizers, fillers, or other additives in the foam. It is also

suggested that the amount of each compound present in the FPUF liquid generated by this method should be quantified via wet chemical analysis techniques. Furthermore, more information should be obtained on the exact strain of *B. diminuta* and *C. daeguensis* that were able to degrade TDA in the first 24 hours of the incubation period. Furthermore, the byproducts generated by these species should also be studied. This information can be important for ecological systems contaminated by aromatic diamines.



## 5 Reference List

- (1) Dalinghaus. *What is Polyurethane (Definition, History, & Foundation Repair)*. 2022. <https://www.dalinghausconstruction.com/> (accessed January 25, 2023).
- (2) American Chemistry Council. *Polyurethane Applications*. 2005. <https://www.americanchemistry.com/> (accessed 20 July, 2022).
- (3) ChemEurope. *Polyurethane*. 1997. <https://www.chemeurope.com/en/> (accessed 25 January, 2023).
- (4) Akindoyo, J. O.; Beg, M. D. H.; Ghazali, S.; Islam, M. R.; Jeyaratnam, N.; Yuvaraj, A. R. Polyurethane types, synthesis and applications – a review. *RSC Advances* **2016**, 6 (115), 114453-114482, 10.1039/C6RA14525F. DOI: 10.1039/C6RA14525F.
- (5) Bottom paint store. *The Many Uses of Polyurethane Paint and Coatings*. 2022. <https://www.bottompaintstore.com/> (accessed 2 February, 2023).
- (6) Akfix. What Is A Polyurethane Sealant? Where And How To Use? 2021; Vol. 10 March, 2023.
- (7) Stokes, K.; McVenes, R.; Anderson, J. M. Polyurethane Elastomer Biostability. *Journal of Biomaterials Applications* **1995**, 9 (4), 321-354. DOI: 10.1177/088532829500900402.
- (8) S&P Global. *Polyurethane Elastomers*. 2020. <https://www.spglobal.com/commodityinsights/en> (accessed 10 March, 2023).
- (9) Petrović, Z. S.; Ferguson, J. Polyurethane elastomers. *Progress in Polymer Science* **1991**, 16 (5), 695-836. DOI: [https://doi.org/10.1016/0079-6700\(91\)90011-9](https://doi.org/10.1016/0079-6700(91)90011-9).
- (10) Vantage Market Research. *Global Polyurethane Market to Worth USD 91.2 Billion by 2028*. GlobeNewswire, 2023. <https://www.globenewswire.com/> (accessed 1 February, 2023).
- (11) Statista. *Market volume of polyurethane worldwide from 2015 to 2025, with a forecast for 2022 to 2029*. Lucía Fernández, 2022. <https://www.statista.com/> (accessed 1 February, 2023).
- (12) Precedence Research. *Polyurethane Market Size, Trends, Share, Growth, Report 2030*. 2023. <https://www.precedenceresearch.com/> (accessed 1 February, 2023).
- (13) Guo, L.; Wang, W.; Guo, X.; Hao, K.; Liu, H.; Xu, Y.; Liu, G.; Guo, S.; Bai, L.; Ren, D.; et al. Recycling of Flexible Polyurethane Foams by Regrinding Scraps into Powder to Replace Polyol for Re-Foaming. *Materials* **2022**, 15 (17), 6047.

- (14) Amundarain, I.; Miguel-Fernández, R.; Asueta, A.; García-Fernández, S.; Arnaiz, S. Synthesis of Rigid Polyurethane Foams Incorporating Polyols from Chemical Recycling of Post-Industrial Waste Polyurethane Foams. *Polymers* **2022**, *14* (6), 1157.
- (15) Das, A.; Mahanwar, P. A brief discussion on advances in polyurethane applications. *Advanced Industrial and Engineering Polymer Research* **2020**, *3* (3), 93-101. DOI: <https://doi.org/10.1016/j.aiepr.2020.07.002>.
- (16) Savelyev, Y.; Veselov, V.; Markovskaya, L.; Savelyeva, O.; Akhranovich, E.; Galatenko, N.; Robota, L.; Travinskaya, T. Preparation and characterization of new biologically active polyurethane foams. *Materials Science and Engineering C* **2014**, *45*, 127-135, Article. DOI: 10.1016/j.msec.2014.08.068 Scopus.
- (17) R.J, L. Manufacture of MDI-TDI based flexible polyurethane foams. 2006.
- (18) Szycher, M. *Szycher's Handbook of Polyurethanes*; 2012. DOI: <https://doi.org/10.1201/b12343>.
- (19) Demharter, A. Polyurethane rigid foam, a proven thermal insulating material for applications between +130°C and -196°C. *Cryogenics* **1998**, *38* (1), 113-117. DOI: [https://doi.org/10.1016/S0011-2275\(97\)00120-3](https://doi.org/10.1016/S0011-2275(97)00120-3).
- (20) Park, K.-M.; Min, K.-S.; Roh, Y.-S. Design Optimization of Lattice Structures under Compression: Study of Unit Cell Types and Cell Arrangements. *Materials* **2022**, *15* (1), 97.
- (21) Kaikade, D. S.; Sabnis, A. S. Polyurethane foams from vegetable oil-based polyols: a review. *Polym Bull (Berl)* **2023**, *80* (3), 2239-2261. DOI: 10.1007/s00289-022-04155-9 From NLM.
- (22) Waleed, H. Q.; Csécsi, M.; Hadjadj, R.; Thangaraj, R.; Pecsmány, D.; Owen, M.; Szőri, M.; Fejes, Z.; Viskolcz, B.; Fiser, B. Computational Study of Catalytic Urethane Formation. *Polymers (Basel)* **2021**, *14* (1). DOI: 10.3390/polym14010008 From NLM.
- (23) Yan, M.; Li, Y. Study on the synthesis of organosilicon foam stabilizers for rigid polyurethane foams. **2005**, 30-33.
- (24) Klempner, D.; Sendjarević, V.; Aseeva, R. M. *Handbook of polymeric foams and foam technology*; Hanser Publishers, 2004.
- (25) Association, P. F. *What is Flexible Polyurethane Foam*. 2022. <https://www.pfa.org/legal-notice/> (accessed 6 February, 2023).
- (26) Bakalo, L. A.; Sirotinskaya, A. L.; Lipatova, T. E.; Blagonravova, A. A.; Pronina, I. A. The reaction kinetics of urethane formation in the presence of metal compounds and tertiary amines. *Polymer Science U.S.S.R.* **1973**, *15* (1), 104-109, Article. DOI: 10.1016/0032-3950(73)90271-2 Scopus.

- (27) Lefebvre, J.; Bastin, B.; Le Bras, M.; Duquesne, S.; Paleja, R.; Delobel, R. Thermal stability and fire properties of conventional flexible polyurethane foam formulations. *Polymer Degradation and Stability* **2005**, *88* (1), 28-34. DOI: <https://doi.org/10.1016/j.polymdegradstab.2004.01.025>.
- (28) Liang, C.; Gracida-Alvarez, U. R.; Gallant, E. T.; Gillis, P. A.; Marques, Y. A.; Abramo, G. P.; Hawkins, T. R.; Dunn, J. B. Material Flows of Polyurethane in the United States. *Environmental Science & Technology* **2021**, *55* (20), 14215-14224. DOI: 10.1021/acs.est.1c03654.
- (29) Alavi Nikje, M. M. *Recycling of Polyurethane Wastes*; De Gruyter, 2019. DOI: 10.1515/9783110641592.
- (30) Yang, W.; Dong, Q.; Liu, S.; Xie, H.; Liu, L.; Li, J. Recycling and Disposal Methods for Polyurethane Foam Wastes. *Procedia Environmental Sciences* **2012**, *16*, 167-175. DOI: <https://doi.org/10.1016/j.proenv.2012.10.023>.
- (31) DeGaspari, J. From Trash to Cash. *Mechanical Engineering* **1999**, *121* (06), 48-51. DOI: 10.1115/1.1999-jun-1 (accessed 3/19/2023).
- (32) American Chemical Council. *Center for the Polyurethanes Industry (CPI)*. 2005. <https://www.americanchemistry.com/> (accessed 23 December, 2022).
- (33) Kemonia, A.; Piotrowska, M. Polyurethane Recycling and Disposal: Methods and Prospects. *Polymers (Basel)* **2020**, *12* (8). DOI: 10.3390/polym12081752 From NLM.
- (34) Zia, K. M.; Bhatti, H. N.; Ahmad Bhatti, I. Methods for polyurethane and polyurethane composites, recycling and recovery: A review. *Reactive and Functional Polymers* **2007**, *67* (8), 675-692. DOI: <https://doi.org/10.1016/j.reactfunctpolym.2007.05.004>.
- (35) Kemonia, A.; Piotrowska, M. Polyurethane Recycling and Disposal: Methods and Prospects. *Polymers* **2020**, *12* (8), 1752.
- (36) Członka, S.; Bertino, M. F.; Strzelec, K.; Strąkowska, A.; Masłowski, M. Rigid polyurethane foams reinforced with solid waste generated in leather industry. *Polymer Testing* **2018**, *69*, 225-237. DOI: <https://doi.org/10.1016/j.polymertesting.2018.05.013>.
- (37) Magnin, A.; Pollet, E.; Perrin, R.; Ullmann, C.; Persillon, C.; Phalip, V.; Avérous, L. Enzymatic recycling of thermoplastic polyurethanes: Synergistic effect of an esterase and an amidase and recovery of building blocks. *Waste Management* **2019**, *85*, 141-150. DOI: <https://doi.org/10.1016/j.wasman.2018.12.024>.
- (38) Ketata, N.; Sanglar, C.; Waton, H.; Alamercery, S.; Delolme, F.; Raffin, G.; Grenier-Loustalot, M. F. Thermal Degradation of Polyurethane Bicomponent Systems in Controlled Atmospheres. *Polymers and Polymer Composites* **2005**, *13* (1), 1-26. DOI: 10.1177/096739110501300101.

- (39) Chao, C. Y. H.; Wang, J. H. Comparison of the thermal decomposition behavior of a non-fire retarded and a fire retarded flexible polyurethane foam with phosphorus and brominated additives. *Journal of Fire Sciences* **2001**, *19* (2), 137-156, Article. DOI: 10.1106/Q56W-KUDB-0VRT-6HLF Scopus.
- (40) Font, R.; Fullana, A.; Caballero, J.; Candela, J.; García, A. Pyrolysis study of polyurethane. *Journal of Analytical and Applied Pyrolysis* **2001**, *58*, 63-77. DOI: 10.1016/S0165-2370(00)00138-8.
- (41) Bloch, E. D.; Queen, W. L.; Krishna, R.; Zdrozny, J. M.; Brown, C. M.; Long, J. R. Hydrocarbon separations in a metal-organic framework with open iron(II) coordination sites. *Science* **2012**, *335* (6076), 1606-1610. DOI: 10.1126/science.1217544 From NLM.
- (42) Huang, K.; Wang, S.; Sun, M.; Tang, L. Techno-Economic Comparison and Analysis of a Novel NGL Recovery Scheme with Three Patented Schemes. *The Open Petroleum Engineering Journal* **2017**, *10*, 19-28. DOI: 10.2174/1874834101701010019.
- (43) Chemical Industry, D. Covestro Partners with French Firm on Chemical Recycling of Polyurethane Foam. *Chemical industry digest (Mumbai)* **2021**.
- (44) Aguado, A.; Martínez, L.; Moral, A.; Feroso, J.; Irusta, R. Chemical recycling of polyurethane foam waste via glycolysis. *Chemical engineering transactions* **2011**, *24*, 1069-1074. DOI: 10.3303/CET1124179.
- (45) Gerlock, J. L.; Braslaw, J.; Mahoney, L. R.; Ferris, F. C. Reaction of polyurethane foam with dry steam: Kinetics and mechanism of reactions. *Journal of Polymer Science: Polymer Chemistry Edition* **1980**, *18* (2), 541-557. DOI: <https://doi.org/10.1002/pol.1980.170180215>.
- (46) Wang, G.; Lopez, L.; Coile, M.; Chen, Y.; Torkelson, J. M.; Broadbelt, L. J. Identification of Known and Novel Monomers for Poly(Hydroxyurethanes) from Biobased Materials. *Ind. Eng. Chem. Res.* **2021**, *60*, 6814.
- (47) Mahoney, L. R.; Weiner, S. A.; Ferris, F. C. Hydrolysis of polyurethane foam waste. *Environmental Science & Technology* **1974**, *8* (2), 135-139. DOI: 10.1021/es60087a010.
- (48) United States Environmental Protection Agency. *Flame Retardants Used in Flexible Polyurethane Foam*. 2015. <https://www.epa.gov/> (accessed).
- (49) Simón, D.; Borreguero, A. M.; de Lucas, A.; Rodríguez, J. F. Recycling of Polyurethanes from Laboratory to Industry, a Journey towards the Sustainability. *Waste Manage.* **2018**, *76*, 147.
- (50) Yang, L. S.; Macarevich, D. A. Hydrolysis of polyurethanes. U.S. Patent 5208379. 1992.

- (51) Molero, C.; de Lucas, A.; Rodríguez, J. F. Recovery of polyols from flexible polyurethane foam by “split-phase” glycolysis with new catalysts. *Polymer Degradation and Stability* **2006**, *91* (4), 894-901. DOI: <https://doi.org/10.1016/j.polymdegradstab.2005.06.023>.
- (52) Wu, C. H.; Chang, C. Y.; Cheng, C. M.; Huang, H. C. Glycolysis of waste flexible polyurethane foam. *Polymer Degradation and Stability* **2003**, *80* (1), 103-111, Article. DOI: 10.1016/S0141-3910(02)00390-7 Scopus.
- (53) Bauer, G. Recycling and recovery of plastics. *Recycling of Polyurethanes* **1996**, 518-537, Article. Scopus.
- (54) Simioni, F.; Modesti, M. Glycolysis of flexible polyurethane foams. *Cellular Polymers* **1993**, *12* (5), 337-348, Article. Scopus.
- (55) Borda, J.; Pásztor, G.; Zsuga, M. Glycolysis of polyurethane foams and elastomers. *Polymer Degradation and Stability* **2000**, *68* (3), 419-422, Article. DOI: 10.1016/S0141-3910(00)00030-6 Scopus.
- (56) Bukowski, A.; Grętkiewicz, J. Polyurethane synthesis reactions in asphalts. *Journal of Applied Polymer Science* **1982**, *27* (4), 1197-1204. DOI: <https://doi.org/10.1002/app.1982.070270409>.
- (57) Carrera, V.; Cuadri, A. A.; García-Morales, M.; Partal, P. Influence of the prepolymer molecular weight and free isocyanate content on the rheology of polyurethane modified bitumens. *European Polymer Journal* **2014**, *57*, 151-159, Article. DOI: 10.1016/j.eurpolymj.2014.05.013 Scopus.
- (58) Gupta, P.; Bhandari, S. 6 - Chemical Depolymerization of PET Bottles via Ammonolysis and Aminolysis. In *Recycling of Polyethylene Terephthalate Bottles*, Thomas, S., Rane, A., Kanny, K., V.K, A., Thomas, M. G. Eds.; William Andrew Publishing, 2019; pp 109-134.
- (59) Lentz, H.; Mormann, W. Chemical recycling of polyurethanes and separation of the components by supercritical ammonia. *Makromolekulare Chemie. Macromolecular Symposia* **1992**, *57* (1), 305-310. DOI: <https://doi.org/10.1002/masy.19920570127>.
- (60) Bhandari, S.; Gupta, P. Chemical Depolymerization of Polyurethane Foam via Ammonolysis and Aminolysis. Elsevier, 2018; pp 1-1.
- (61) Sheratte, M. B. Process for converting the decomposition products of polyurethane and novel compositions thereby obtained. U.S. Patent 4110266, 1978.
- (62) Lenntech. *Chemical elements listed by electronegativity*. 1998. <https://www.lenntech.com/> (accessed 6 April, 2023).

- (63) Rahm, M.; Erhart, P.; Cammi, R. Relating atomic energy, radius and electronegativity through compression. *Chemical Science* **2021**, *12* (7), 2397-2403, 10.1039/D0SC06675C. DOI: 10.1039/D0SC06675C.
- (64) Todar, K. Nutrition and Growth of Bacteria. In *Todar's Online Textbook of Bacteriology*, 2020.
- (65) Thakor, N. S.; Patel, M. A.; Trivedi, U. B.; Patel, K. C. Production of poly( $\beta$ -hydroxybutyrate) by *Comamonas testosteroni* during growth on naphthalene. *World journal of microbiology & biotechnology* **2003**, *19* (2), 185-189. DOI: 10.1023/A:1023295009846.
- (66) Blakley, E. R. The microbial degradation of cyclohexanecarboxylic acid by a beta-oxidation pathway with simultaneous induction to the utilization of benzoate. *Can J Microbiol* **1978**, *24* (7), 847-855. DOI: 10.1139/m78-141 From NLM.
- (67) Rho, E. M.; Evans, W. C. The aerobic metabolism of cyclohexanecarboxylic acid by *Acinetobacter anitratum*. *Biochem J* **1975**, *148* (1), 11-15. DOI: 10.1042/bj1480011 From NLM.
- (68) Whitby, C. Chapter 3 - Microbial Naphthenic Acid Degradation. In *Advances in Applied Microbiology*, Vol. 70; Academic Press, 2010; pp 93-125.
- (69) Demeter, M. A.; Lemire, J. A.; Yue, G.; Ceri, H.; Turner, R. J. Culturing oil sands microbes as mixed species communities enhances ex situ model naphthenic acid degradation. *Front Microbiol* **2015**, *6*, 936. DOI: 10.3389/fmicb.2015.00936 From NLM.
- (70) Brenner, K.; You, L.; Arnold, F. H. Engineering microbial consortia: a new frontier in synthetic biology. *Trends Biotechnol* **2008**, *26* (9), 483-489. DOI: 10.1016/j.tibtech.2008.05.004 From NLM.
- (71) Hays, S. G.; Patrick, W. G.; Ziesack, M.; Oxman, N.; Silver, P. A. Better together: engineering and application of microbial symbioses. *Curr Opin Biotechnol* **2015**, *36*, 40-49. DOI: 10.1016/j.copbio.2015.08.008 From NLM.
- (72) Bhatia, S. K.; Bhatia, R. K.; Choi, Y. K.; Kan, E.; Kim, Y. G.; Yang, Y. H. Biotechnological potential of microbial consortia and future perspectives. *Crit Rev Biotechnol* **2018**, *38* (8), 1209-1229. DOI: 10.1080/07388551.2018.1471445 From NLM.
- (73) Cao, Z.; Yan, W.; Ding, M.; Yuan, Y. Construction of microbial consortia for microbial degradation of complex compounds. *Frontiers in Bioengineering and Biotechnology* **2022**, *10*, Review. DOI: 10.3389/fbioe.2022.1051233.
- (74) Larson, E. A.; Lee, J.; Paulson, A.; Lee, Y. J. Structural Analysis of Polyurethane Monomers by Pyrolysis GC TOFMS via Dopant-Assisted Atmospheric Pressure

Chemical Ionization. *Journal of The American Society for Mass Spectrometry* **2019**, 30 (6), 1046-1058. DOI: 10.1007/s13361-019-02165-y.

(75) Utomo, R. N. C.; Li, W.-J.; Tiso, T.; Eberlein, C.; Doeker, M.; Heipieper, H. J.; Jupke, A.; Wierckx, N.; Blank, L. M. Defined Microbial Mixed Culture for Utilization of Polyurethane Monomers. *ACS Sustainable Chemistry & Engineering* **2020**, 8 (47), 17466-17474. DOI: 10.1021/acssuschemeng.0c06019.

(76) Wierckx, N.; Prieto, M. A.; Pomposiello, P.; de Lorenzo, V.; O'Connor, K.; Blank, L. M. Plastic waste as a novel substrate for industrial biotechnology. *Microbial Biotechnology* **2015**, 8 (6), 900-903. DOI: <https://doi.org/10.1111/1751-7915.12312>.

(77) Franden, M. A.; Jayakody, L. N.; Li, W.-J.; Wagner, N. J.; Cleveland, N. S.; Michener, W. E.; Hauer, B.; Blank, L. M.; Wierckx, N.; Klebensberger, J.; et al. Engineering *Pseudomonas putida* KT2440 for efficient ethylene glycol utilization. *Metabolic Engineering* **2018**, 48, 197-207. DOI: <https://doi.org/10.1016/j.ymben.2018.06.003>.

(78) Krooneman, J.; Faber, F.; Alderkamp, A. C.; Oude Elferink, S. J. H. W.; Driehuis, F.; Cleenwerck, I.; Swings, J.; Gottschal, J. C.; Vancanneyt, M. *Lactobacillus diolivorans* sp. nov., a 1,2-propanediol-degrading bacterium isolated from aerobically stable maize silage. *Int. J. Syst. Evol. Microbiol.* **2002**, 52 (2), 639-646, Article. DOI: 10.1099/00207713-52-2-639 Scopus.

(79) Daneshvar, S.; Behrooz, R.; Kazemi, S.; Mir Mohamad Sadeghi, G. Characterization of polyurethane wood adhesive prepared from liquefied sawdust by ethylene carbonate. *BioResources* **2019**, 14, 796-815. DOI: 10.15376/biores.14.1.796-815.

(80) Shah, S. I. A.; Kostiuk, L. W.; Kresta, S. M. The Effects of Mixing, Reaction Rates, and Stoichiometry on Yield for Mixing Sensitive Reactions—Part I: Model Development. *International Journal of Chemical Engineering* **2012**, 2012, 750162. DOI: 10.1155/2012/750162.

(81) Tartakovsky, A. M.; Tartakovsky, G. D.; Scheibe, T. D. Effects of incomplete mixing on multicomponent reactive transport. *Advances in Water Resources* **2009**, 32 (11), 1674-1679. DOI: <https://doi.org/10.1016/j.advwatres.2009.08.012>.

(82) Jiao, L.; Xiao, H.; Wang, Q.; Sun, J. Thermal degradation characteristics of rigid polyurethane foam and the volatile products analysis with TG-FTIR-MS. *Polymer Degradation and Stability* **2013**, 98 (12), 2687-2696. DOI: <https://doi.org/10.1016/j.polymdegradstab.2013.09.032>.

(83) Silverstein, R. M.; Bassler, G. C. Spectrometric identification of organic compounds. *Journal of Chemical Education* **1962**, 39 (11), 546. DOI: 10.1021/ed039p546.

- (84) Williams, M.; Todd, G. D.; Pohl, H. R.; Taylor, J.; Ingerman, L.; Carlson-Lynch, H.; Hard, C.; Citra, M. J. Toxicological profile for toluene diisocyanate and methylenediphenyl diisocyanate. 2018.
- (85) Gili, P.; Mederos, A. On the Toxicity of the Aromatic Diamines and their Tetramethylcarboxylic Acid Derivatives. *Revista de la Sociedad Química de México* **2000**, *44*.
- (86) Li, W. J.; Narancic, T.; Kenny, S. T.; Niehoff, P. J.; O'Connor, K.; Blank, L. M.; Wierckx, N. Unraveling 1,4-Butanediol Metabolism in *Pseudomonas putida* KT2440. *Front Microbiol* **2020**, *11*, 382. DOI: 10.3389/fmicb.2020.00382 From NLM.
- (87) Shi, Y. n.; Li, R.; Zheng, J.; Xue, Y.; Tao, Y.; Yu, B. High-Yield Production of Propionate from 1,2-Propanediol by Engineered *Pseudomonas putida* KT2440, a Robust Strain with Highly Oxidative Capacity. *Journal of Agricultural and Food Chemistry* **2022**, *70* (51), 16263-16272. DOI: 10.1021/acs.jafc.2c06405.
- (88) Inoue, A.; Horikoshi, K. A *Pseudomonas* thrives in high concentrations of toluene. *Nature* **1989**, *338* (6212), 264-266. DOI: 10.1038/338264a0.



## 6 Appendix

### 6.1 Solubilization Data of FPUF in $\text{NH}_4\text{OH}$

#### 6.1.1 Batch Reactor Run Data

Table 6.1: Solubilization triplicate data of FPUF reactions in a batch reactor.  
Reaction conditions: 30, 60 minutes; 140°C, 160°C, 180°C, 200°C; 16% w/w  $\text{NH}_4\text{OH}$ ;  
6.25% FPUF in  $\text{NH}_4\text{OH}$ .

Temperature (°C)	Pressure (psi)	Time (min)	Mass of PUF loaded (g)	Solubilization (%)
140	50	30	0.5059	5
			0.5088	5.6
			0.4981	6.7
160	100	30	0.5043	14.9
			0.4997	17.8
			0.5033	18.1
180	150	30	0.504	44.1
			0.5078	45.9
			0.503	47.7
200	200	30	0.5024	49.9
			0.5042	51.3
			0.4991	53.9
140	50	60	0.5012	19.2
			0.4988	19.9
			0.5023	20
160	100	60	0.4994	27.2
			0.4954	29.1
			0.4967	29.2
180	150	60	0.4989	48.1
			0.5034	49.2
			0.5021	50
200	200	60	0.4979	51.68
			0.5015	53.22
			0.5039	55.35

### 6.1.2 Parr Reactor Run Data

Table 6.2: Solubilization triplicate data of FPUF reactions in a continuously stirred-tank reactor (Parr reactor). Reaction conditions: 30, 60 minutes; 140°C, 160°C, 180°C, 200°C; 60 rpm; 16% w/w NH<sub>4</sub>OH; 6.25% FPUF in NH<sub>4</sub>OH.

Temperature (°C)	Pressure (psi)	Time (min)	Mass of PUF loaded (g)	Solubilization (%)
140	50	30	0.4997	30.5
			0.5024	31.4
			0.5067	34.9
160	100	30	0.5032	44.3
			0.5061	47.1
			0.5049	47.7
180	150	30	0.5024	69.6
			0.5085	72.5
			0.5043	75.3
200	200	30	0.5037	93.3
			0.5078	95.6
			0.4991	96.9
140	50	60	0.5041	36.8
			0.5032	37.7
			0.4997	39.5
160	100	60	0.5039	51.1
			0.5049	51.6
			0.5033	56.4
180	150	60	0.5085	74.7
			0.4987	76.8
			0.5023	82
200	200	60	0.5037	93.6
			0.5015	96
			0.5019	97.4

### 6.1.3 Higher Solids Loading Experimental Data

Table 6.3: Average solubilization data of FPUF decomposition reaction at higher solids loading. Reaction conditions: Reaction conditions: 60 minutes; 200°C; 60 rpm in a Parr reactor; 16% w/w NH<sub>4</sub>OH.

Temperature (°C)	Time (minutes)	Solids loading (%)	Solubilization (%)	Average solubilization (%)
200	30	6.25	96.8	95.3
			93.6	
			95.5	
		10	92.9	93.8
			92.0	
			96.4	
		15	95.3	92.6
			93.1	
			89.2	
		20	93.0	91.9
			92.2	
			90.4	
		25	92.0	91.3
			90.7	
			91.1	
		30	75.9	75.5
			78.1	
			72.3	

## 6.2 Microbial Growth Data (OD<sub>600</sub>)

### 6.2.1 OD<sub>600</sub> During Incubation Period of Microbial Consortia in FPUF Media with 2.3 g/L Dissolved Carbon Products

Table 6.4: OD<sub>600</sub> of microbial consortia in FPUF media. Media specifications: 52 mL media; 2.3 g/L dissolved carbon products; media neutralized to pH = 6.81.

Microbial Consortia	Time (hours)	OD <sub>600</sub> replicates			Average	Microbe OD (Average OD - Media OD)
		1	2	3		
Laura 1	1	0.31	0.3	0.33	0.31	0.29
	2	0.3	0.33	0.29	0.31	0.29
	6	0.32	0.31	0.33	0.32	0.30
	24	0.27	0.26	0.29	0.27	0.25
	48	0.25	0.26	0.24	0.25	0.23
	72	0.23	0.24	0.21	0.23	0.21
	96	0.22	0.21	0.21	0.21	0.19
	120	0.23	0.2	0.21	0.21	0.19
Laura 2	1	0.33	0.31	0.3	0.31	0.30
	2	0.32	0.3	0.29	0.30	0.29
	6	0.33	0.31	0.3	0.31	0.30
	24	0.28	0.27	0.26	0.27	0.26
	48	0.24	0.25	0.25	0.25	0.24
	72	0.23	0.25	0.24	0.24	0.23
	96	0.21	0.22	0.22	0.22	0.21
	120	0.2	0.23	0.22	0.22	0.21
Emma 2	1	0.33	0.33	0.32	0.33	0.30
	2	0.32	0.32	0.31	0.32	0.29
	6	0.33	0.35	0.32	0.33	0.30
	24	0.37	0.39	0.35	0.37	0.34
	48	0.35	0.36	0.34	0.35	0.32
	72	0.29	0.32	0.31	0.31	0.28
	96	0.27	0.28	0.27	0.27	0.24
	120	0.24	0.23	0.25	0.24	0.21

## 6.2.2 OD<sub>600</sub> During Incubation Period of Microbial Consortia in FPUF Liquid Media with 8.8 g/L Dissolved Carbon Products

Table 6.5: Table A.4: OD<sub>600</sub> of microbial consortia in FPUF media. Media specifications: 52 mL media; 8.8 g/L dissolved carbon products; media neutralized to pH = 6.75.

Microbial Consortia	Time (hours)	OD <sub>600</sub> replicates			Average	Microbe OD (Average OD - Media OD)
		1	2	3		
Laura 1	1	0.31	0.31	0.32	0.31	0.30
	2	0.31	0.3	0.32	0.31	0.30
	6	0.3	0.28	0.32	0.30	0.29
	24	0.28	0.27	0.29	0.28	0.27
	48	0.27	0.26	0.27	0.27	0.26
	72	0.25	0.25	0.24	0.25	0.24
	96	0.23	0.22	0.24	0.23	0.22
	120	0.21	0.21	0.23	0.22	0.21
Laura 2	1	0.32	0.32	0.31	0.32	0.30
	2	0.32	0.32	0.31	0.32	0.30
	6	0.33	0.33	0.31	0.32	0.30
	24	0.29	0.29	0.28	0.29	0.27
	48	0.28	0.27	0.26	0.27	0.25
	72	0.26	0.26	0.25	0.26	0.24
	96	0.25	0.24	0.25	0.25	0.23
	120	0.24	0.25	0.25	0.25	0.23
Emma 2	1	0.28	0.3	0.28	0.29	0.29
	2	0.29	0.29	0.28	0.29	0.29
	6	0.32	0.31	0.33	0.32	0.32
	24	0.36	0.35	0.36	0.36	0.36
	48	0.33	0.36	0.34	0.34	0.34
	72	0.31	0.31	0.29	0.30	0.30
	96	0.28	0.26	0.25	0.26	0.26
	120	0.25	0.23	0.24	0.24	0.24

## 7 Copyright Documentation

All images in this document are from open access articles licensed for reuse under Creative Commons license 4.0. Please see below for full citation and attribution information.

Figure 7.1: Closed-cell structure of rigid polyurethane foam (RPUF). Licensed under CC by MDPI, Basel, Switzerland. Park, K.-M.; Min, K.-S.; Roh, Y.-S. Design Optimization of Lattice Structures under Compression: Study of Unit Cell Types and Cell Arrangements. *Materials* **2022**, *15*, 97. <https://doi.org/10.3390/ma15010097>

Figure 7.2: Open-celled structure of flexible polyurethane foam (FPUF). Licensed under CC by MDPI, Basel, Switzerland. Park, K.-M.; Min, K.-S.; Roh, Y.-S. Design Optimization of Lattice Structures under Compression: Study of Unit Cell Types and Cell Arrangements. *Materials* **2022**, *15*, 97. <https://doi.org/10.3390/ma15010097>